

Validation of Geotechnical Computer Program “3d-DMM (SPH Version 2.0)”

GEO Report No. 353

R.P.H. Law, J.S.H. Kwan & F.W.Y. Ko

**Geotechnical Engineering Office
Civil Engineering and Development Department
The Government of the Hong Kong
Special Administrative Region**

[Blank Page]

Validation of Geotechnical Computer Program “3d-DMM (SPH Version 2.0)”

GEO Report No. 353

R.P.H. Law, J.S.H. Kwan & F.W.Y. Ko

**This report was originally produced in May 2016
as GEO Technical Note No. TN 3/2016**

© The Government of the Hong Kong Special Administrative Region

First published, March 2022

Prepared by:

Geotechnical Engineering Office,
Civil Engineering and Development Department,
Civil Engineering and Development Building,
101 Princess Margaret Road,
Homantin, Kowloon,
Hong Kong.

Preface

In keeping with our policy of releasing information which may be of general interest to the geotechnical profession and the public, we make available selected internal reports in a series of publications termed the GEO Report series. The GEO Reports can be downloaded from the website of the Civil Engineering and Development Department (<http://www.cedd.gov.hk>) on the Internet.



Raymond WM Cheung
Head, Geotechnical Engineering Office
March 2022

Foreword

This Technical Note presents the details of the validation exercise of the core calculation module of the geotechnical computer program, 3d-DMM (SPH Version 2.0).

The validation exercise was carried out by Dr R.P.H. Law, under the supervision of Dr J.S.H. Kwan, Ms F.W.Y. Ko and myself. Technical Officer, Ms C.C.Y. Cheung, and Summer Intern, Mr H.Y. Tang, provided valuable assistance in the validation exercise. The Drafting Unit of the Standards and Testing Division assisted in formatting this report. All contributions are gratefully acknowledged.



H.W. Sun

Chief Geotechnical Engineer/Standards and Testing

Abstract

Two-dimensional modelling of landslide motions has been routinely used to assess landslide mobility in natural terrain hazard studies. With the advance in digital and computer technology, 3-dimensional modelling of landslide motions is not uncommon. The 3-dimensional modelling module, 3d-DMM (SPH Version 1.0), was developed in 2010 based on the numerical technique of smoothed particle hydrodynamics (SPH) that operates on the Microsoft Excel platform.

Three dimensional simulations of landslide debris mobility require pre-processing and post-processing of a large amount of three dimensional spatial data. In order to enhance its efficiency in performing three dimensional landslide mobility analyses, 3d-DMM (SPH Version 1.0) has recently been revamped to 3d-DMM (SPH Version 2.0) that operates on the ArcGIS platform.

The validation exercise of 3d-DMM (SPH Version 2.0) includes a comparison of results of back-analyses of six historical landslides with the field velocity and runout data. It is demonstrated that 3d-DMM (SPH Version 2.0) produced results that were consistent with the field data/observations.

Contents

	Page No.
Title Page	1
Preface	3
Foreword	4
Abstract	5
Contents	6
List of Tables	8
List of Figures	9
1 Introduction	10
2 Introduction of Smoothed Particle Hydrodynamics (SPH)	10
2.1 Equations of Motion	10
2.2 Method of SPH	12
2.3 Calculation of Tangential Earth Pressure Coefficient, k	14
2.4 Velocity Smoothing	15
2.5 Difference between 3d-DMM (SPH) and DAN-3D	16
2.6 Calculation of Distance between Smoothed Particles	16
3 Key Improvements	17
4 Validation of 3d-DMM (SPH Version 2.0)	17
5 Key Findings	19
6 Conclusions	20
7 References	20
Appendix A: Summary of Input Parameters Adopted in 3d-DMM (SPH Version 2.0), 3d-DMM (PIC Version), 2d-DMM (Version 2.0) and LS-DYNA	21
Appendix B: Effects of Apparent Internal Friction Angle, Smoothing Coefficient (B) and Time Step on Simulation Results	25

Appendix C: Detailed Input and Output of the Validation Exercise

34

List of Tables

Table No.		Page No.
4.1	Summary of Cases in the Validation Exercise	18

List of Figures

Figure No.		Page No.
2.1	Summation of Interplant Given by Particles within Influence Zone	13

1 Introduction

Two-dimensional modelling of landslide motions has been routinely used to assess landslide mobility in natural terrain hazard studies in Hong Kong. With the advance in digital and computer technology, 3-dimensional modelling of landslide motions is not uncommon. Back in the late 2000s, Kwan & Sun (2007) adopted the Particle-in-Cell (PIC) numerical technique to solve the governing equations to simulate 3-dimensional landslide debris mobility. The PIC numerical technique is similar to the material point method reported by Soga et al (2016). Another 3-dimensional modelling module, 3d-DMM (SPH Version 1.0), based on smoothed particle hydrodynamics (SPH) that operates on the Microsoft Excel platform was developed in 2010. 3d-DMM (SPH Version 1.0) performs time marching analysis and produces a series of result files in Excel format. These files are then visualised using the Surfer (Version 8).

Three dimensional simulations of landslide debris mobility require pre-processing and post-processing of a large amount of three dimensional spatial data. In order to enhance its efficiency in performing three dimensional landslide mobility analyses, 3d-DMM (SPH Version 1.0) has recently been revamped to 3d-DMM (SPH Version 2.0) that operates on the ArcGIS platform.

The newly developed 3d-DMM (SPH Version 2.0) program operates on an improved Graphical User Interface which guides users through defining a problem, solving the problem through SPH modelling and analysing the simulation results on the ArcGIS platform in a seamless manner. The core calculation module of 3d-DMM (SPH Version 2.0) has also been improved over the original 3d-DMM (SPH Version 1.0) program by using optimised internal data storage algorithm which enhances the computation efficiency.

This Technical Note presents the details of the validation exercise of the core calculation module of 3d-DMM (SPH Version 2.0).

2 Introduction of Smoothed Particle Hydrodynamics (SPH)

2.1 Equations of Motion

Landslide debris is considered as an equivalent fluid in setting up the equations of motion. The equations of motion follow the mass and momentum conservations presented below:

Mass Conservation:

$$\frac{\partial h}{\partial t} + h \left(\frac{\partial u}{\partial x} + \frac{\partial v}{\partial y} \right) = \frac{\partial b}{\partial t} \dots\dots\dots (2.1)$$

Momentum Conservation in x-direction:

$$\rho h \frac{\partial u}{\partial t} = \rho g_x h - k_x \sigma_z \left(\frac{\partial h}{\partial x} \right) + \tau_{xbed} - \rho u \frac{\partial b}{\partial t} \dots\dots\dots (2.2)$$

Momentum Conservation in y-direction:

$$\rho h \frac{\partial v}{\partial t} = \rho g_y h - k_y \sigma_z \left(\frac{\partial h}{\partial y} \right) + \tau_{ybed} - \rho v \frac{\partial b}{\partial t} \dots\dots\dots (2.3)$$

- where
- x = the direction of motion
 - y = the direction perpendicular to the x and z axes
 - z = the direction normal to the channel base
 - u = velocity component in the x direction
 - v = velocity component in the y direction
 - ρ = debris density
 - g_x = gravity acceleration in the x direction
 - g_y = gravity acceleration in the y direction
 - σ_z = bed-normal earth pressure
 - h = debris depth
 - k_x = tangential earth pressure coefficient in the x direction
 - k_y = tangential earth pressure coefficient in the y direction
 - τ_{xbed} = basal shear stress in the x direction
 - τ_{ybed} = basal shear stress in the y direction
 - b = bed-normal erosion-entrainment depth.

According to McDougall (2006), the bed-normal erosion-entrainment depth, b , is also known as the “erosion velocity”. The erosion-entrainment depth is considered to be positive during erosion. The erosion-entrainment depth must be adjusted by trial-and-error in order to obtain a reasonable distribution of entrained material.

In Equations 2.2 and 2.3, the terms on the left-hand side of the momentum equations represent the debris accelerations in the respective directions, the first term on the right-hand side relates to the body force, and the second term represents the internal pressure arising from the effect of the debris depth gradient. The third term (τ_{xbed} and τ_{ybed}) in the momentum conservation equations represents the base friction against the debris motion, which depends on the rheology of the debris. The last term in the momentum conservation equations represents the change of momentum due to entrainment. Ayotte & Hungr (1998) studied 20 landslides and debris flows in Hong Kong. They showed that Voellmy rheological model (Equations 2.4 and 2.5) produces reasonable estimate for the base friction.

$$\tau_{xbed} = - Sgn(u) \left[\sigma_z \tan \phi + \frac{u^2}{\zeta} \right] \dots\dots\dots (2.4)$$

$$\tau_{ybed} = - Sgn(v) \left[\sigma_z \tan \phi + \frac{v^2}{\zeta} \right] \dots\dots\dots (2.5)$$

- where
- ϕ = Apparent basal friction angle at the debris base
 - ξ = Voellmy coefficient which account for the turbulent loss during the landslide motions
 - σ_z = bed-normal earth pressure
 - u = velocity component in the x direction
 - v = velocity component in the y direction
 - τ_{xbed} = basal shear stress in the x direction
 - τ_{ybed} = basal shear stress in the y direction.

The $Sgn(x)$ function in Equations 2.4 and 2.5 is defined as follows:

$$Sgn(x) = \begin{cases} +1 ; x > 0 \\ 0 ; x = 0 \\ -1 ; x < 0 \end{cases} \dots\dots\dots (2.6)$$

3d-DMM (SPH Version 2.0) adopts the Saint-Vanent approximation to simplify the calculation of motion of landslide debris. The assumptions of shallow flow and smooth flow path, relative to the flow thickness, are implicit in modelling debris mobility using 3d-DMM (SPH Version 2.0). Therefore, 3d-DMM (SPH Version 2.0) is not suitable for simulation of debris dynamics involving abrupt change in slope gradient.

2.2 Method of SPH

McDougall & Hungr (2004) adopted SPH to develop a numerical model for simulation of debris motions. Each of the particles in this method has a finite volume (V_i), and bears an influence zone defined by an interpolation kernel (W). Properties such as debris depth and velocity at any location can be estimated by summation of the interplant of particles within the local influence radius. For example, the total debris thickness, h_i , at the position of particle i , is calculated as:

$$h_i = V_i \sum_{j=1}^n W(s_{ij}, l) \dots\dots\dots (2.7)$$

- where
- s_{ij} = distance between particle i and j
 - l = radius of the influence zone.

The interpolating kernel, W , is a function of s_{ij} and l . s_{ij} is the separation distance between the particle i and particle j , which is within the influence zone of the particle i . The radius of the influence zone is l . The summation is undertaken for all particles (i.e. $j = 1$ to n) within the influence zone (Figure 2.1).

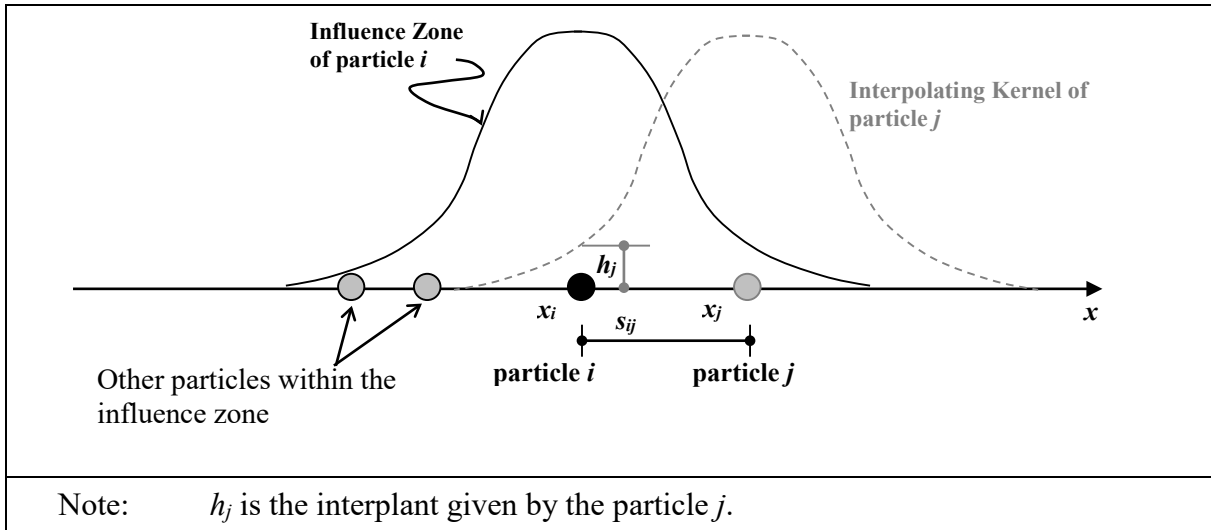


Figure 2.1 Summation of Interplant Given by Particles within Influence Zone

The kernel is represented by the following Gaussian function:

$$W(s_{ij}, l) = \frac{1}{\pi l^2} \exp \left[- \left(\frac{s_{ij}}{l} \right)^2 \right] \dots\dots\dots (2.8)$$

l , the radius of the influence zone, is defined as follows:

$$l = \frac{B}{\sqrt{\frac{\sum_{i=1}^N h_i}{N}}} \dots\dots\dots (2.9)$$

- where
- B = smoothing coefficient, taken as 10 by McDougall & Hungr (2004)
 - V = volume of the smoothed particle i
 - N = total number of particles used for representing the whole debris mass
 - s_{ij} = distance between particle i and j
 - l = radius of the influence zone
 - h_i = total debris thickness at the position of particle i .

The debris depth gradient at particle i can be obtained as follows:

$$\left(\frac{\partial h}{\partial x} \right)_i = \sum_{j=1}^n V_j \left| \frac{\partial W}{\partial s} \right|_{ij} \frac{x_{ij}}{\sqrt{x_{ij}^2 + y_{ij}^2}} \dots\dots\dots (2.10)$$

$$\left(\frac{\partial h}{\partial y} \right)_i = \sum_{j=1}^n V_j \left| \frac{\partial W}{\partial s} \right|_{ij} \frac{y_{ij}}{\sqrt{x_{ij}^2 + y_{ij}^2}} \dots\dots\dots (2.11)$$

$$\left| \frac{\partial W}{\partial s} \right|_{ij} = \frac{2s_{ij}}{\pi l^4} \exp \left[- \left(\frac{s_{ij}}{l} \right)^2 \right] \dots\dots\dots (2.12)$$

- where
- h_i = total debris thickness at the position of particle i
 - j = index of particles within the influence zone of particle i
 - W_{ij} = kernel of particle i and j
 - s_{ij} = distance between particle i and j
 - x_{ij} = x component of the distance between particle i and j
 - y_{ij} = y component of the distance between particle i and j
 - l = radius of the influence zone
 - V_j = the volume of particle j .

With the above Equations 2.7 to 2.12, the debris thickness and depth gradient can be calculated at each of the particles considered in the simulation. Having calculated debris thickness and depth gradient, acceleration of each of the particles can be obtained based on the momentum conservation equation. The simulation is undertaken in a time-stepping framework with an initial condition that all the particles are at rest. At each time step, the velocities of the particles are updated based on the acceleration calculated via the momentum conservation equation, and the particles are displaced to new positions.

There are special cases where the influence between smoothed particles located within the influence zone are not reasonable. For example, two separate clusters of smoothed particles, travelling on different but close drainage channels, will have their thickness and acceleration averaged with each other, which is not permissible in reality.

2.3 Calculation of Tangential Earth Pressure Coefficient, k

As in the Rankine theory, the tangential earth pressure coefficients (i.e. k_x and k_y shown in Equations 2.2 and 2.3 respectively) are limited by the Mohr Coulumb failure criterion. The minimum and maximum limiting values correspond to the “active” and “passive” states, respectively. The limits of the tangential earth pressure coefficient are calculated using the following equations, after Savage & Hutter (1989):

$$k_{x(\min/\max)} = 2 \left\{ \frac{1 \pm \sqrt{1 - \cos^2 \phi_i \left(1 + \left(\frac{\tau_{bed}}{\sigma_z} \right)^2 \right)}}{\cos^2 \phi_i} \right\} - 1 \dots\dots\dots (2.13)$$

$$k_{y(\min)} = \left[\left(\frac{k_x + 1}{2} \right) + \sqrt{\left(\frac{k_x - 1}{2} \right)^2 + \left(\frac{\tau_{bed}}{\sigma_z} \right)^2} \right] \left(\frac{1 - \sin \phi_i}{1 + \sin \phi_i} \right) \dots\dots\dots (2.14)$$

$$k_{y(\max)} = \left[\left(\frac{k_x + 1}{2} \right) + \sqrt{\left(\frac{k_x - 1}{2} \right)^2 + \left(\frac{\tau_{bed}}{\sigma_z} \right)^2} \right] \left(\frac{1 + \sin \phi_i}{1 - \sin \phi_i} \right) \dots\dots\dots (2.15)$$

where k_x = tangential earth pressure coefficient in the x direction
 k_y = tangential earth pressure coefficient in the y direction
 ϕ_i = Apparent internal friction angle¹ of the landslide debris
 τ_{bed} = base friction against the debris motion
 σ_z = bed-normal earth pressure.

According to McDougall & Hungr (2004), the axes of principal stress is assumed to align with the direction of motion. Also, the local x axis align with the direction of motion, in order to eliminate the transverse stress and momentum terms in the governing momentum equations.

In the formation proposed by McDougall & Hungr (2004), the k value is incremented at each time step in proportion to the corresponding incremental strain (Hungr, 1995), up to the limiting values of Equations 2.13 to 2.15. The k_x and k_y value is calculated using the following equations.

$$k_x = k_x' + C(\Delta\varepsilon_x) \dots\dots\dots (2.16)$$

$$k_y = k_y' + C(\Delta\varepsilon_y) \dots\dots\dots (2.17)$$

where k_x' and k_y' are the tangential earth pressure coefficient in x and y directions respectively in the previous time step, and C is the dimensionless stiffness coefficient. The k_x and k_y values are taken as 1.0 at time equals zero.

2.4 Velocity Smoothing

According to McDougall (2006), a velocity smoothing is applied to the updated velocities of smoothed particles to minimise the excessive relative motion between neighbouring smoothed particles, especially in the absence of viscosity.

$$u_i = u_i + C_s(\Delta u_i) \dots\dots\dots (2.18)$$

$$v_i = v_i + C_s(\Delta v_i) \dots\dots\dots (2.19)$$

where u_i and v_i are the velocity of smoothed particle i in x and y directions respectively, C_s is the user-specified velocity smoothing coefficient, and Δu_i and Δv_i are the following velocity correction:

¹ By adopting the Saint-Venant approximation, the SPH model does not use the apparent internal friction angle to calculate the internal shear stress due to deformation. The apparent internal friction angle is only used to calculate the k_x and k_y

$$\Delta u_i = \sum_{j=1}^n \frac{V_j}{\left(\frac{h_i+h_j}{2}\right)} (u_j - u_i) W_{ij} \dots\dots\dots (2.20)$$

$$\Delta v_i = \sum_{j=1}^n \frac{V_j}{\left(\frac{h_i+h_j}{2}\right)} (v_j - v_i) W_{ij} \dots\dots\dots (2.21)$$

where V_j is the volume of smoothed particle j ; W_{ij} is the kernel between particle i and j calculated by Equation 2.8, h_i and h_j are the total debris thickness at the position of particle i and j respectively.

2.5 Difference between 3d-DMM (SPH) and DAN-3D

It should be noted that the method of calculating k in 3d-DMM (SPH Version 2.0) is different from that of DAN-3D, the SPH package for debris mobility analysis developed by Prof. O. Hungr based on McDougall & Hungr (2004). In 3d-DMM (SPH Version 2.0), the incremental tangential strains in the major and minor principle axes, $\Delta\varepsilon_x$ and $\Delta\varepsilon_y$, are calculated in each time step. The major principle axis is assumed aligning with the direction of motion. The active state (i.e. minimum lateral earth pressure coefficient, k_{\min}) is assumed when the $\Delta\varepsilon$ is smaller than 0 whereas the passive state (i.e. maximum lateral earth pressure coefficient, k_{\max}) is assumed when the $\Delta\varepsilon$ is larger than 0. The lateral earth pressure coefficient corresponding to the at-rest state (i.e. k_0 ; k_0 assumed to be 1.0) is adopted if $\Delta\varepsilon$ equals 0.

$$k_{x \text{ or } y} = \begin{cases} k_{(x \text{ or } y)\min} & \text{if } \Delta\varepsilon_{(x \text{ or } y)} < 0 \\ k_{(x \text{ or } y)\max} & \text{if } \Delta\varepsilon_{(x \text{ or } y)} > 0 \end{cases} \dots\dots\dots (2.22)$$

Also, in 3d-DMM (SPH Version 2.0), the particle velocity is not adjusted using the velocity smoothing function (i.e. Equations 2.18 and 19).

2.6 Calculation of Distance between Smoothed Particles

The distances between each smoothed particles are calculated in each time step for the calculation of the kernel (Equation 2.8) and the depth gradient (Equations 2.10 to 2.12). It is a classical fixed-radius near neighbours problem. In 3d-DMM (SPH Version 2.0), such problem is solved by the “brute-force approach” which calculates all pair-wise distances of particles. Such approach is efficient when the number of particles are limited. In cases where over 10,000 particles are involved, alternative algorithms such as cell-linked list or Verlet list (Dominguez et al, 2011) can be used. These alternative approach should be used with caution since they can increase memory usage and introduce calculation errors.

3 Key Improvements

The followings are the key improvements made in 3d-DMM (SPH Version 2.0):

- (a) A Graphical User Interface (GUI) has been developed to guide users through defining a problem, solving the problem through SPH modelling and analysing the simulation results on the ArcGIS platform; and
- (b) The core calculation module has been improved by using a better internal data storage algorithm which reduces the computation time approximately by half. For example, the time required for 3d-DMM (Version 2.0) to simulate the landslide event of Verification Case No. 1 is less than one hour, which is faster than that of 3d-DMM (Version 1.0) which take more than two hours.

4 Validation of 3d-DMM (SPH Version 2.0)

Table 4.1 shows six historical landslides (Verification Cases No. 1 to 6) that were used in the validation exercise of 3d-DMM (SPH Version 2.0). All of the six historical landslides are Hong Kong cases. They include three channelised debris flows, viz. Yu Tung Road landslide, Sham Tseng San Tsuen landslide and 1990 Tsing Shan landslide, a landslide which travelled in a topographic depression, viz. Kau Lung Hang Shan landslide, and two open hillside failures, viz. Fei Tsui Road landslide and Shum Wan landslide.

The results of 3d-DMM (SPH Version 2.0) were compared with field data/observations and outputs of other geotechnical computer programmes on landslide mobility (e.g. 2d-DMM (Version 2.0)) if available.

It has been shown that 3d-DMM (SPH Version 2.0) is capable of producing simulations that match generally the field data/observations based on the rheological parameters similar to those adopted by other debris mobility programmes including DAN-3D. Appendix A summarises the rheological parameters adopted, Appendix B details a sensitivity study of the key input parameters adopted in 3d-DMM (SPH Version 2.0) and Appendix C presents the results of each of the validation cases.

It should be emphasised again that 3d-DMM (SPH Version 2.0) adopts Saint-Venant approximation. The flow path cannot contain any abrupt change in slope gradient in order for the approximation to be valid.

Table 4.1 Summary of Cases in the Validation Exercise

Summary Table										
Case No.	Case	Source Volume (m ³)	Density (kg/m ³)	Apparent Basal Friction Angle (°)	Apparent Internal Friction Angle ⁽¹⁾⁽⁴⁾ (°)	Turbulent Coefficient (m/s ²)	Smoothing Coefficient ⁽¹⁾	Comparison with Field Observations	Comparison with 2d-DMM (Version 2.0)	Remarks
1	Yu Tung Road landslide	2,600	2,200	8	30	500	4	✓	✓	Channelised debris flow
2	Sham Tseng San Tsuen landslide	600	2,200	8	30	500	4	✓	✓	Channelised debris flow
3	1990 Tsing Shan landslide	4,000	2,200	15	30	500	4	✓	✓	Channelised debris flow with entrainment. Final volume = 20,000 m ³
4	Kau Lung Hang Shan landslide	180	2,200	17	30	1000	4	✓	✓	Debris flow travelled in topographic depression
5	Fei Tsui Road landslide	14,000	2,200	22 / 35 ⁽²⁾	30	0 ⁽³⁾	4	✓		Open hillside failure
6	Shum Wan landslide	26,000	2,200	19	33	0 ⁽³⁾	4	✓		Open hillside failure

- Notes:
- ⁽¹⁾ Please refer to Appendix B for the sensitivity study of the apparent internal friction angle and the smoothing coefficient.
 - ⁽²⁾ The apparent friction angle = 22° for landslide source area and 35° for movement of the landslide debris over Fei Tsui Road.
 - ⁽³⁾ Friction model is adopted in the simulation, and therefore turbulent coefficient = 0.
 - ⁽⁴⁾ By adopting the Saint-Venant approximation, the SPH model does not use the apparent internal friction angle to calculate the internal shear stress due to deformation. The apparent internal friction angle is only used to calculate the k_x and k_y .

5 Key Findings

The key findings of the validation exercise are discussed below.

- (a) As shown in Verification Cases No. 1, 2 and 3, the results between the field velocity data and the simulated velocity profiles against time are in general consistent. Also, for Verification Cases No. 1 to 4, the velocity profiles computed using 3d-DMM (SPH Version 2.0) and 2d-DMM (Version 2.0) are in reasonably well agreement with each other. The computed deposition profile fits with the measured one for Verification Case No. 3. However, while the same set of apparent basal friction angle and turbulent coefficient are adopted in Verification Case No. 1 for the 2d- and 3d-DMM, there are slight differences in the apparent basal friction angles adopted by 2d-DMM (Version 2.0) and 3d-DMM (SPH Version 2.0) in Verification Cases No. 2, 3 and 4. The differences in the apparent basal friction angles for back analysis are probably due to the difference in the method of discretisation between the two computer programs.
- (b) As shown in Verification Cases No. 5 and 6, the measured and computed deposit profiles of the open hillside failures are in general consistent. Also, the deposit extent simulated using 3d-DMM (SPH Version 2.0) also match reasonably well with the computed deposit profiles reported by Kwan & Sun (2007) using 3d-DMM (PIC Version). *(It should be noted that the computed program presented by Kwan & Sun (2007) is currently not a pre-accepted computed program and the comparison between the two computer programs could therefore be considered as reference only.)* The values of the apparent internal friction angle adopted in the back analysis of Verification Cases No. 1 to 5 are the same and are equal to 30° , which is the recommended value elaborated in the sensitivity study presented in Appendix B. A slightly larger apparent internal friction angle, 33° , was back-calculated for Verification Case No. 6 in order to match the observed debris deposition profile.
- (c) The computed results of 3d-DMM (SPH Version 2.0) is in general consistent with that of the LS-DYNA.
- (d) In all cases, the smoothing coefficient (i.e. B value) and the time step was taken as 4 and 0.01 s respectively. These values are the recommended values elaborated in the sensitivity study presented in Appendix B.

6 Conclusions

The validation exercise demonstrates that the core calculation module of 3d-DMM (SPH Version 2.0) produces results that are consistent with the field data/observations of selected landslide cases, the computed results of 2d-DMM (Version 2.0) and other debris mobility programs.

7 References

- Ayotte, D. & Hungr, O. (1998). *Runout Analysis of Debris Flows and Debris Avalanches in Hong Kong*. A Report for the Geotechnical Engineering Office, Hong Kong. University of British Columbia, Canada, 90 p.
- Dominguez, J.M., Crespo, A.J.C., Gómez-Gesteira, M. & Marongiu, J.C. (2011). Neighbour lists in smoothed particle hydrodynamics. *International Journal for Numerical Methods in Fluids*, vol. 67, issue no. 12, pp 2026-2042.
- Hungr, O. (1995). A model for the runout analysis of rapid flow slides, debris flows and avalanches. *Canadian Geotechnical Journal*, vol. 32, pp 610-623.
- Kwan, J.S.H. & Sun, H.W. (2007). Benchmarking exercise on landslide mobility modelling - runout analyses using 3dDMM. *Proceedings of the 2007 International Forum on Landslide Disaster Management*, Hong Kong, pp 945-966.
- McDougall, S. (2006). *A New Continuum Dynamic Model for the Analysis of Extremely Rapid Landslide Motion Across Complex 3D Terrain* (Doctoral dissertation, University of British Columbia).
- McDougall, S. & Hungr, O. (2004). A model for the analysis of rapid landslide motion across three-dimensional terrain. *Canadian Geotechnical Journal*, vol. 41, pp 1084-1097.
- Savage, S.B. & Hutter, K. (1989). The motion of a finite mass of granular material down a rough incline. *Journal of Fluid Mechanics*, vol. 199, pp 177-215.
- Soga, K., Alonso, E., Yerro, A., Kumar, K. & Bandara, S. (2016). Trends in large-deformation analysis of landslide mass movements with particular emphasis on the material point method. *Géotechnique*, no. 66, issue 3, pp 248 - 273. (<http://dx.doi.org/10.1680/jgeot.15.LM.005>)

Appendix A

Summary of Input Parameters Adopted in 3d-DMM (SPH Version 2.0),
3d-DMM (PIC Version), 2d-DMM (Version 2.0) and LS-DYNA

Content

	Page No.
List of Table	23

List of Table

Table No.		Page No.
A1	Summary of Input Parameters Adopted in 3d-DMM (SPH Version 2.0), 3d-DMM (PIC Version), 2d-DMM (Version 2.0) and LS-DYNA	24

Table A1 Summary of Input Parameters Adopted in 3d-DMM (SPH Version 2.0), 3d-DMM (PIC Version), 2d-DMM (Version 2.0) and LS-DYNA

		Apparent Basal Friction Angle (°)	Turbulent Coefficient (m/s ²)
Case No. 1 Yu Tung Road landslide	3d-DMM (SPH Version 2.0)	8	500
	3d-DMM (PIC Version) ⁽²⁾	-	-
	2d-DMM (Version 2.0)	8	500
	LS-DYNA	8	500
	DAN-3D	8	500
Case No. 2 Sham Tseng San Tsuen landslide	3d-DMM (SPH Version 2.0)	8	500
	3d-DMM (PIC Version)	12	500
	2d-DMM (Version 2.0)	11	500
	LS-DYNA	9	250
Case No. 3 ⁽¹⁾ 1990 Tsing Shan landslide	3d-DMM (SPH Version 2.0)	15	500
	3d-DMM (PIC Version)	15	500
	2d-DMM (Version 2.0)	18	700
Case No. 4 ⁽¹⁾ Kau Lung Hang landslide	3d-DMM (SPH Version 2.0)	17	1000
	3d-DMM (PIC Version) ⁽²⁾	-	-
	2d-DMM (Version 2.0)	18	1000
Case No. 5 Fei Tsui landslide	3d-DMM (SPH Version 2.0)	22/35	0
	3d-DMM (PIC Version)	22/35	0
	2d-DMM (Version 2.0) ⁽³⁾	-	-
	LS-DYNA	22/35	0
Case No. 6 Shum Wan landslide	3d-DMM (SPH Version 2.0)	19	0
	3d-DMM (PIC Version)	20	0
	2d-DMM (Version 2.0) ⁽³⁾	-	-
	LS-DYNA	20	0

Notes: ⁽¹⁾ Verification Cases No. 3 and 4 are not covered in Koo (2015).
⁽²⁾ Verification Cases No. 1 and 4 are not covered in Kwan & Sun (2007).
⁽³⁾ Verification Cases No. 5 and 6 are open hillside failures and were not studied using 2d-DMM (Version 2.0).

References

- Koo, R.C.H. (2015). *3D Debris Mobility Assessment Using LS-DYNA (SPR 4/2015)*. Geotechnical Engineering Office, Hong Kong, 87 p.
- Kwan, J.S.H. & Sun, H.W. (2007). An improved landslide mobility model. *Canadian Geotechnical Journal*, vol. 43, pp 531-539.

Appendix B

Effects of Apparent Internal Friction Angle, Smoothing Coefficient (B)
and Time Step on Simulation Results

Contents

	Page No.
List of Figures	27
B.1 Introduction	28
B.2 Apparent Internal Friction Angle	28
B.3 Smoothing Coefficient	30
B.4 Time Step	31
B.5 Recommendations	33
B.6 References	33

List of Figures

Figure No.		Page No.
B1	Comparison of Computed Frontal Velocity Using Different Apparent Internal Frictional Angles (ϕ_i) in Verification Case No. 2	29
B2	Comparison of Computed Average Thickness Using Different Apparent Internal Frictional Angles (ϕ_i) in Verification Case No. 2	29
B3	Comparison of Computed Frontal Velocity Using Different Smoothing Coefficients (B) in Verification Case No. 2	30
B4	Comparison of Computed Average Thickness Using Different Smoothing Coefficients (B) in Verification Case No. 2	31
B5	Comparison of Computed Frontal Velocity Using Different Time Steps in Verification Case No. 5	32
B6	Comparison of Computed Average Depth Time Series Using Different Time Steps in Verification Case No. 5	32
B7	Comparison of Computed Peak Velocity Using Different Time Steps in Verification Case No. 2	33

B.1 Introduction

The sensitivity of apparent internal friction angle (i.e. not used in 2d-DMM), smoothing coefficient (i.e. not used in 2d-DMM) and time step (i.e. different numerical scheme between 2d-DMM and 3d-DMM) on the calculated mobility of landslide debris was assessed. This Appendix presents the findings of the sensitivity study. A set of suggested values of these parameters are also presented based on the study. Verification Cases No. 1, 2, 5 and 6 were used in the sensitivity study.

B.2 Apparent Internal Friction Angle

Apparent internal friction angle (ϕ_i) refers to the total stress (i.e. apparent) friction angle of the assumed homogeneous landslide debris. Figures B1 and B2 illustrate two examples that shows the effect of apparent internal friction angle (ϕ_i) on the computed time history of the peak velocity and average thickness. The peak velocity refers to the average velocity of the smoothed particles which have the top 10% of the tangential velocity at any time step, thus representing the most dynamic part of the landslide debris. The apparent internal friction angle varies at 20°, 25°, 30°, 35° and 40°. The smoothing coefficient (B) and time step (Δt) are fixed at 4 and 0.01 s respectively. Other key input parameters (e.g. apparent basal friction angle) adopted in the sensitivity study follows the values given in Table 4.1. It is observed that both the peak velocity and average thickness of the landslide debris are in general insensitive to the apparent internal friction angle chosen. Based on the findings, a value of 30° for apparent internal friction angle is considered reasonable for the back analysis. It should, however, be noted that the temporal analysis presented above may not reflect the effects of apparent internal friction angle on the longitudinal and lateral spreading of landslide debris. For example, the spreading of the landslide debris in Verification Case No. 6 needs to be restrained by increasing slightly the apparent internal friction angle from 30° to 33° in order to avoid the landslide debris on the shipyard from spreading excessively.

In addition, the Savage-Hutter theory adopted in 3d-DMM (SPH Version 2.0) is valid when the apparent internal friction angle is greater than or equal to the apparent basal friction angle. When the designer determines that an apparent basal friction angle exceeding 30° should be adopted for a landslide simulation, a larger value of apparent internal friction angle should be adopted.

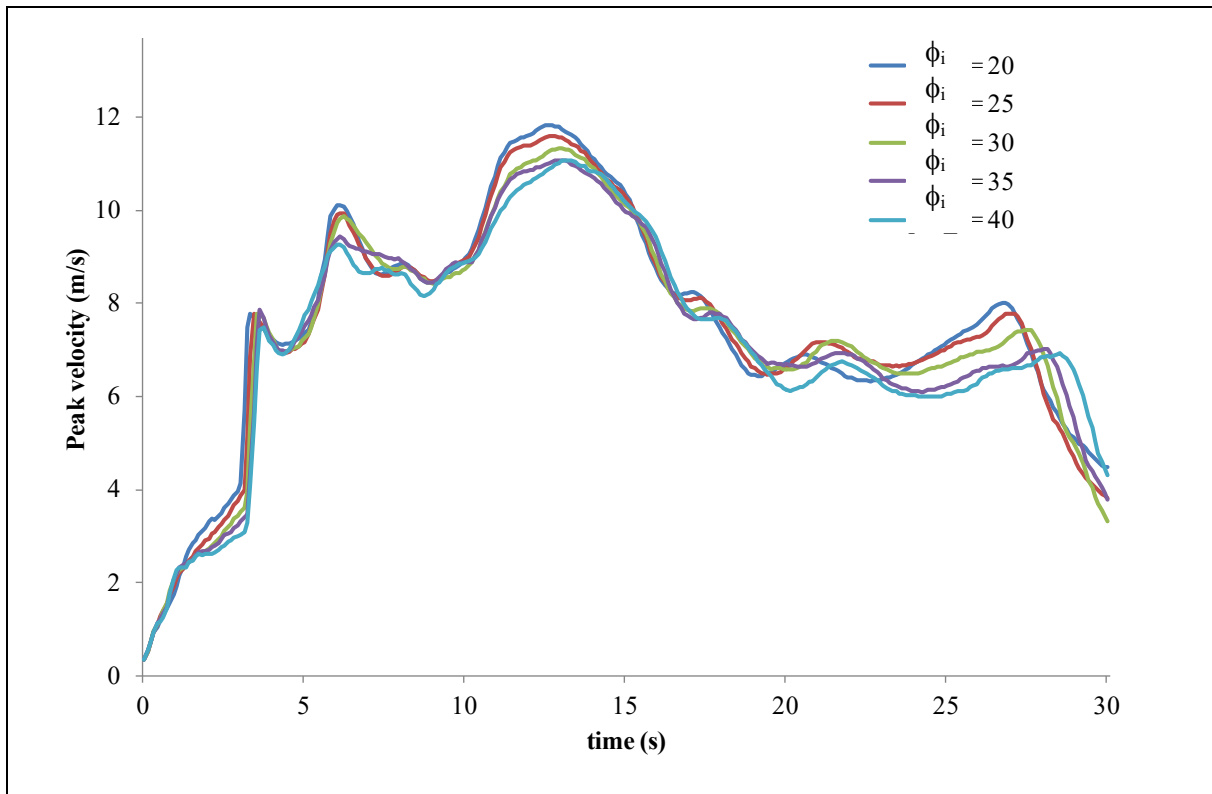


Figure B1 Comparison of Computed Frontal Velocity Using Different Apparent Internal Frictional Angles (ϕ_i) in Verification Case No. 2

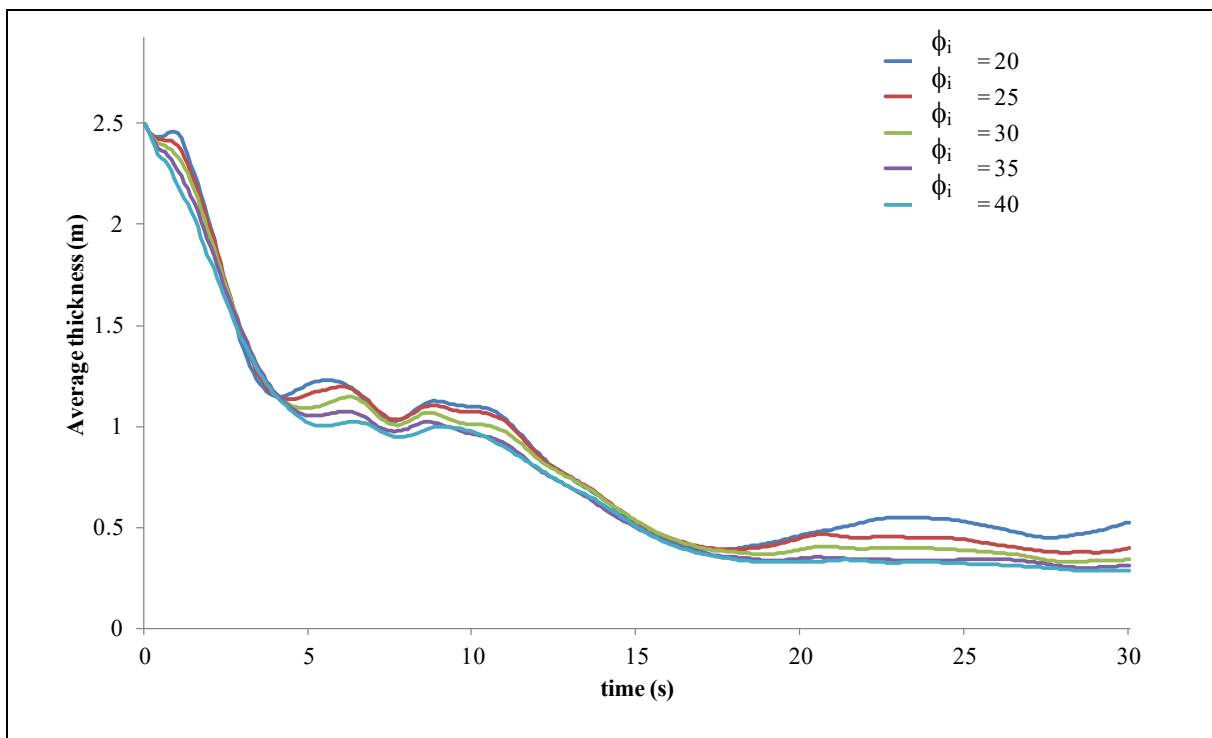


Figure B2 Comparison of Computed Average Thickness Using Different Apparent Internal Frictional Angles (ϕ_i) in Verification Case No. 2

B.3 Smoothing Coefficient

Figures B3 and B4 show two examples of the effects of smoothing coefficient (B) (see Equation 2.9) on the computed frontal velocity and average thickness. Different values of smoothing coefficient were used. The apparent internal friction angle and time step (Δt) are fixed at 30° and 0.01 s respectively. Other input parameters (e.g. apparent basal friction angle) adopted in the sensitivity study follows the values given in Table 4.1. It is noted that a smaller B in general produces a higher flow velocity while its effects on average flow depth is less consistent. It is noted that the time history of frontal velocity converges as the smoothing coefficient decreases to 4.

The observation can be explained by the fact that the velocity values of the frontal particles are the weighted average with the neighbouring particles that follows the debris front (which are usually slower than the debris front). By adopting a large smoothing coefficient, a larger number of slower neighbours are involved in determining the velocity of the frontal particles, thus reducing the calculated debris velocity. Based on the findings, a smoothing coefficient of 4 is considered reasonable for the back analysis. The choice of $B = 4$ is also the recommendation by McDougall & Hungr (2004).

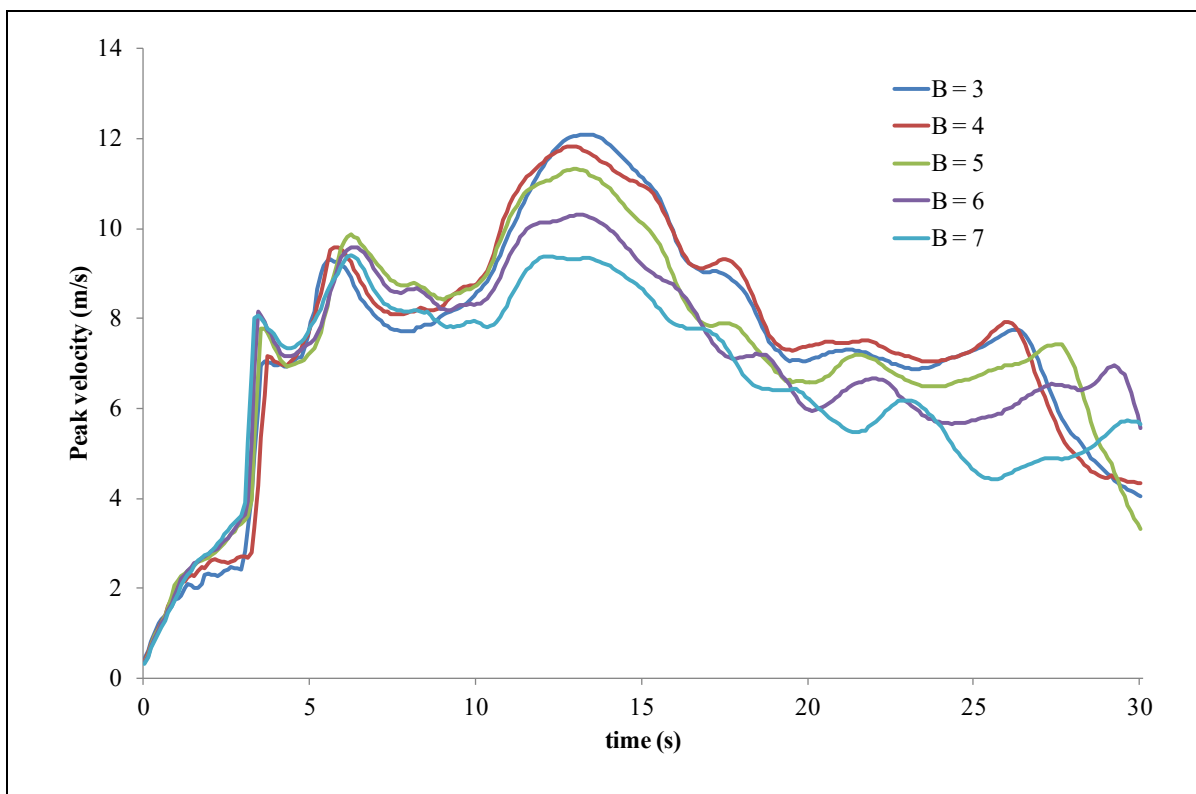


Figure B3 Comparison of Computed Frontal Velocity Using Different Smoothing Coefficients (B) in Verification Case No. 2

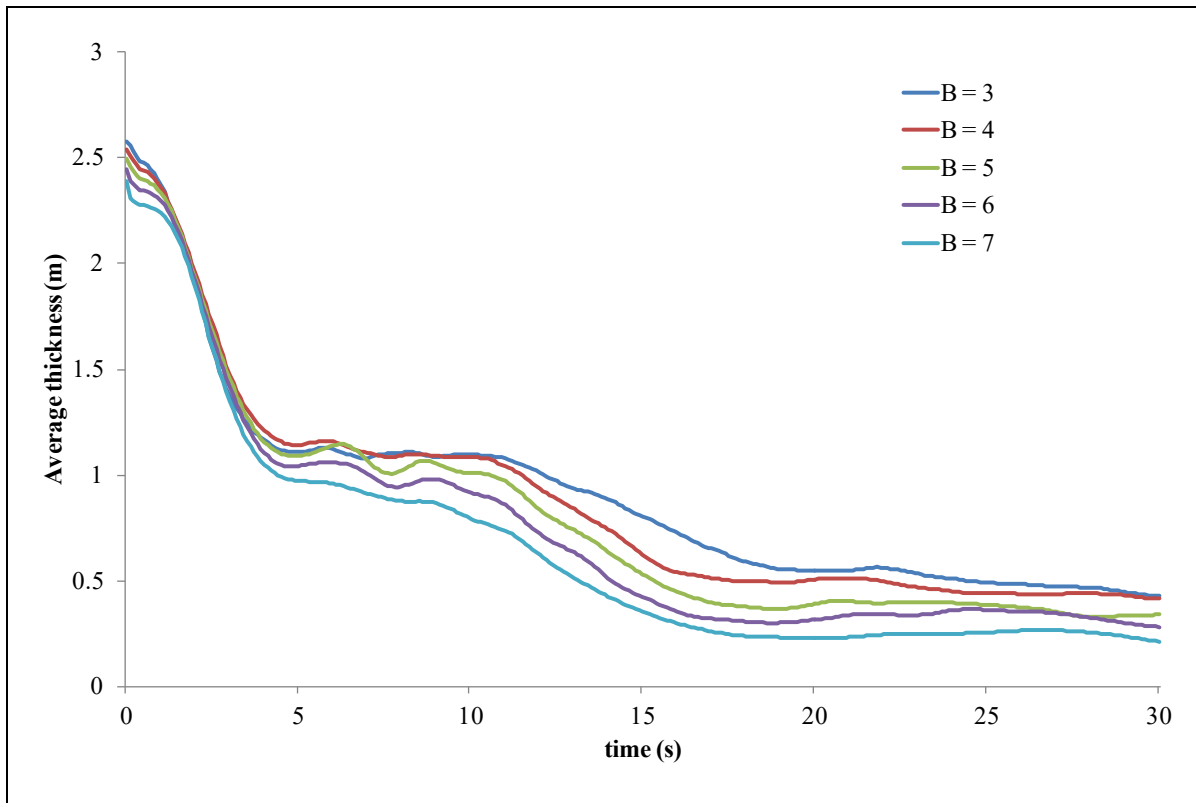


Figure B4 Comparison of Computed Average Thickness Using Different Smoothing Coefficients (B) in Verification Case No. 2

B.4 Time Step

Apart from apparent internal friction angle and smoothing coefficient, a sensitivity study is performed on the time step Δt . Figures B5 and B6 illustrate two examples of the effects of time step (Δt) on the computed peak velocity and average thickness. The time step varies at 0.1 s, 0.05 s and 0.01 s. The apparent internal friction angle and smoothing coefficient are fixed at 30° and 4 respectively. Other input parameters (e.g. apparent basal friction angle) adopted in the sensitivity study follows the values given in Table 4.1. The output files were produced every 0.1 s of prototype time. It is observed that the computed peak velocity decreases with smaller time step, and converges when $\Delta t = 0.01$ s. In contrast, the average thickness is in general insensitive to the change in the time step. It is therefore considered that a time step of 0.01 s or less is appropriate for simulating landslides. However, it is noted in Verification Case No. 2 that the computed peak velocity is insensitive to the three time steps (i.e. 0.1 s, 0.05 s and 0.01 s, see Figure B7). The optimum time step (i.e. the largest time step which, when further reduced, does not influence the computed result) is therefore case specific and should be determined on a case-by-case basis, but $\Delta t = 0.01$ s would generally be small enough to produce reasonable results for typical landslide cases.

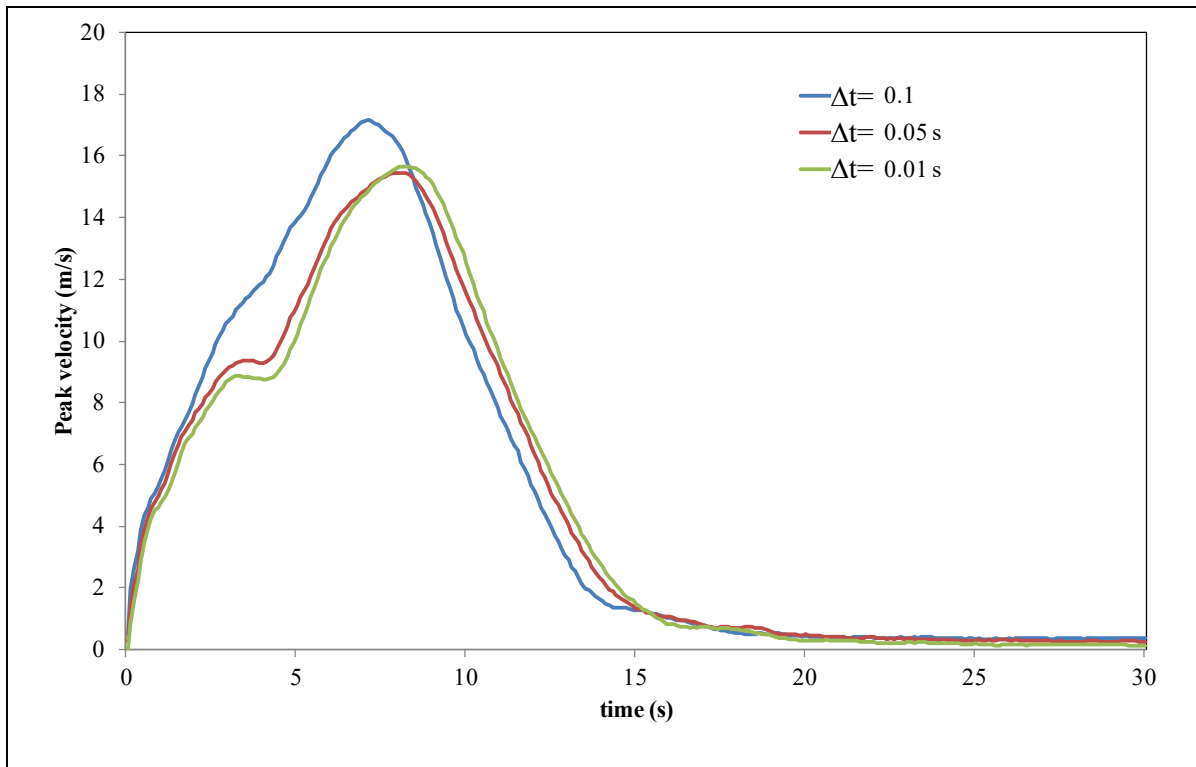


Figure B5 Comparison of Computed Frontal Velocity Using Different Time Steps in Verification Case No. 5

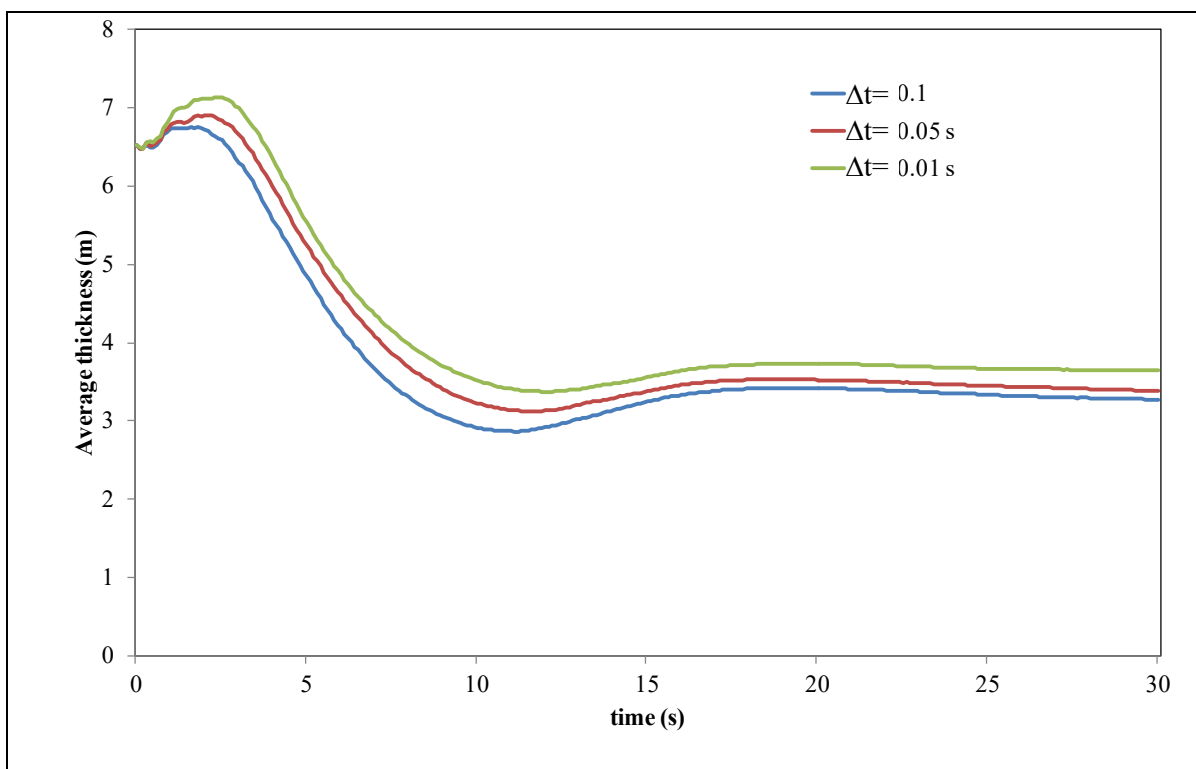


Figure B6 Comparison of Computed Average Depth Time Series Using Different Time Steps in Verification Case No. 5

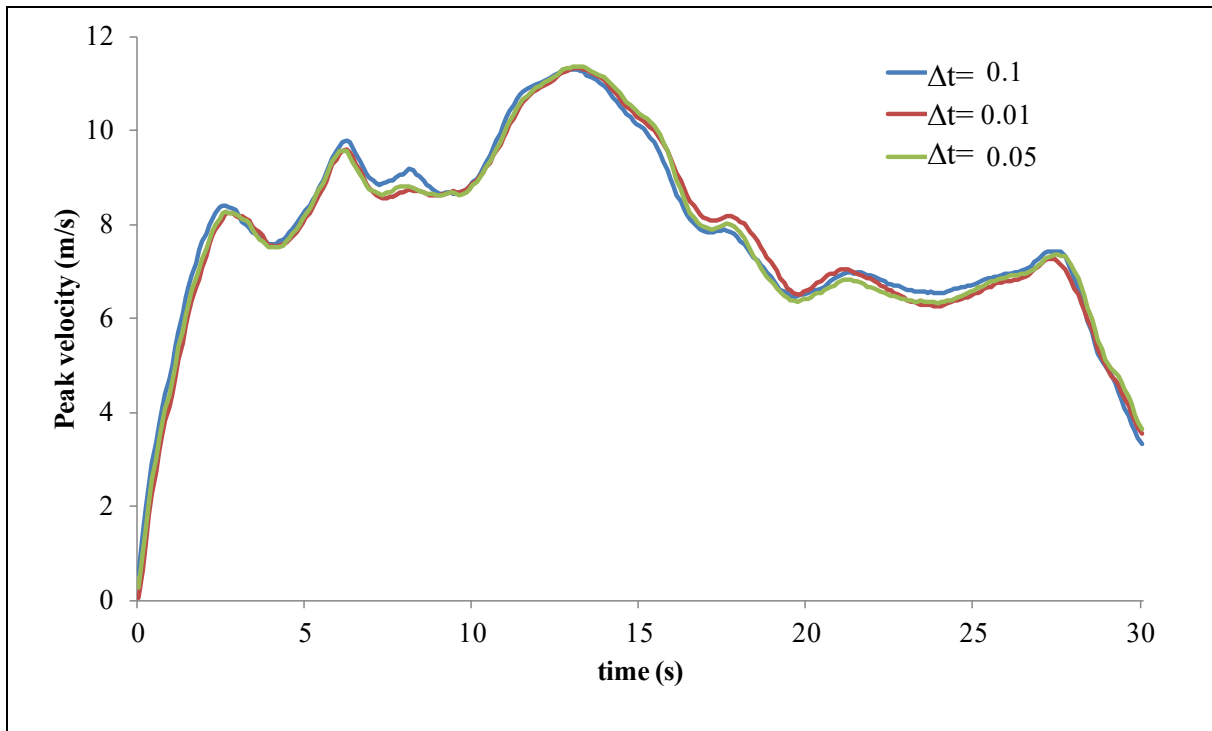


Figure B7 Comparison of Computed Peak Velocity Using Different Time Steps in Verification Case No. 2

B.5 Recommendations

Based on the findings of the sensitivity study discussed above, the following values of apparent internal friction angle, smoothing coefficient and time step are recommended for use in the validation of 3d-DMM (SPH Version 2.0).

- $\phi_i = 30^\circ - 33^\circ$
- $B = 4$
- $\Delta t = 0.01$ s.

B.6 References

McDougall, S. & Hungr, O. (2004). A model for the analysis of rapid landslide motion across three-dimensional terrain. *Canadian Geotechnical Journal*, vol. 41, pp 1084-1097.

Appendix C

Detailed Input and Output of the Validation Exercise

Contents

	Page No.
List of Tables	36
List of Figures	37
C.1 Validation Case No. 1 - Yu Tung Road Landslide	39
C.2 Validation Case No. 2 - Sham Tseng San Tsuen Landslide	43
C.3 Validation Case No. 3 - 1990 Tsing Shan Landslide	46
C.4 Validation Case No. 4 - Kau Lung Hang Shan Landslide	51
C.5 Validation Case No. 5 - Fei Tsui Road Landslide	54
C.6 Validation Case No. 6 - Shum Wan Landslide	58

List of Tables

Table No.		Page No.
C1	Input Parameters Adopted for the Validation Case No. 1	40
C2	Input Parameters Adopted for the Validation Case No. 2	45
C3	Input Parameters Adopted for the Validation Case No. 3	46
C4	Input Parameters Adopted for the Validation Case No. 4	52
C5	Input Parameters Adopted for the Validation Case No. 5	54
C6	Input Parameters Adopted for the Validation Case No. 6	58

List of Figures

Figure No.		Page No.
C1	Comparison between the Computed Velocity Profiles Using 2d-DMM (Version 2.0), 3d-DMM (SPH Version 2.0), LS-DYNA and Field Evidence of Debris Flow above Yu Tung Road in June 2008	39
C2	Debris Frontal Location versus Time Estimated by 3d-DMM (SPH Version 2.0) Analysis	41
C3	Comparison between the Computed Maximum Velocity Profiles Using 3d-DMM (SPH Version 2.0) and DAN-3D	42
C4	Comparison between the Computed Velocity Profiles Using 2d-DMM (Version 2.0), 3d-DMM (SPH Version 2.0) and Field Evidence of Debris Flow above Sham Tseng San Tsuen in August 1999	43
C5	Comparison between the Computed Velocity Profiles Using 2d-DMM (Version 2.0), 3d-DMM (SPH Version 2.0) and Field Observation of Debris Flow on Tsing Shan in September 1990	47
C6(a)	Comparison between the Field Evidence and the Simulated Debris Profiles Using 3d-DMM (SPH Version 2.0)	48
C6(b)	Comparison between the Field Evidence and the Simulated Debris Profiles Using 3d-DMM (PIC Version) (Kwan & Sun, 2007))	49
C7	Comparison between the Computed Velocity Profiles Using 2d-DMM (Version 2.0), 3d-DMM (SPH Version 2.0) and Field Evidence of Debris Flow at Kau Lung Hang Shan Tai Po in 2003	51
C8	Comparison between the Field Evidence (red lines) and the Simulated Debris Profiles Using 3d-DMM (SPH Version 2.0) and 3d-DMM (PIC Version) (Kwan & Sun, 2007))	55
C9	Comparison of Velocity and Thickness of Debris of Fei Tsui Road Landslide Reaching the Southern Corner of the Opposite Church Building with Time	56

Figure No.		Page No.
C10	Comparison between the Field Evidence (red lines) and the Simulated Debris Profiles Using (a) 3d-DMM (SPH Version 2.0) and (b) 3d-DMM (PIC Version) (Kwan & Sun, 2007)	59
C11	Comparison of Simulations between LS-DYNA and 3d-DMM (PIC Version) (Koo, 2015)	60

C.1 Validation Case No. 1 - Yu Tung Road Landslide

The June 2008 Yu Tung Road debris flow event involved a single landslide source. The landslide debris reached Yu Tung Road, resulting in blockage of both westbound lanes and flooding of the adjacent Cheung Tung Road. About 2,600 m³ of debris was involved which had a runout distance of about 600 m, and all the debris reached Yu Tung Road. The lower portion of the channelised debris flow was captured on video by a member of the public, although the exact time of the failure is not known.

Figure C1 shows the velocity profiles of debris front along chainage for Verification Case No. 1. Both the published velocity data from GEO (2012) (shown in dots) and the computed data using both 3d-DMM (SPH Version 2.0) (shown in red dotted line), 2d-DMM (Version 2.0) (shown in green solid line) and LS-DYNA (shown in blue solid line) are presented in the figure. Table C1 presents the input parameters adopted by the two computer programs. In the 3d-DMM (SPH Version 2.0) analysis, the frontal velocity was calculated by the average tangential velocity of the foremost 10% of the smoothed particles that simulate the landslide debris. In the 2d-DMM (Version 2.0) analysis, the velocity of the foremost boundary block represents the frontal velocity of the landslide debris. The same set of the friction angle and the turbulent coefficient were adopted for 3d-DMM (SPH Version 2.0) and 2d-DMM (Version 2.0). It is noted that the frontal velocities calculated using 2d-DMM (Version 2.0), 3d-DMM (SPH Version 2.0) and LS-DYNA match reasonably well with the field data.

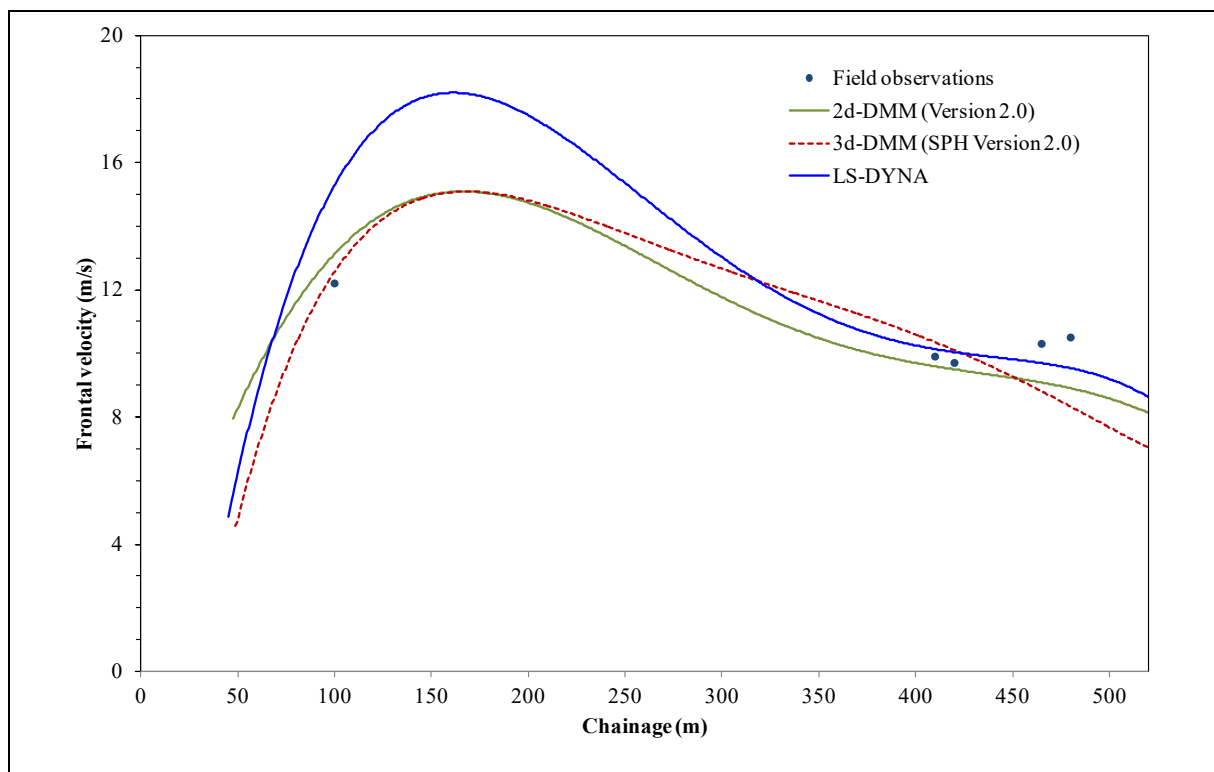


Figure C1 Comparison between the Computed Velocity Profiles Using 2d-DMM (Version 2.0), 3d-DMM (SPH Version 2.0), LS-DYNA and Field Evidence of Debris Flow above Yu Tung Road in June 2008

Table C1 Input Parameters Adopted for the Validation Case No. 1

<i>Input Parameters for 2d-DMM (Version 2.0)</i>					
Debris Properties		Section 1			
Density (kg/m ³):	2,200	Friction angle ⁽¹⁾ (°):	8	Entrainment start location (m):	0
Source volume (m ³):	2,600	Turbulent coefficient (m/s ²):	500	Entrainment end location (m):	0
Initial horizontal length of flow mass (m):	50	Pore pressure for friction:	0	Entrainment rate (m ³ /s):	0
K_a :	0.8	Section 2			
K_θ :	1	Start location of section 2 (m):	1,000	Entrainment start location (m):	0
K_p :	2.5	Friction angle (°):	8	Entrainment end location (m):	0
Pore pressure ratio (R_u):	0.5	Turbulent coefficient (m/s ²):	500	Entrainment rate (m ³ /s):	0
Initial location of landslide debris (m):	0	Pore pressure for friction:	0		
Initial velocity (m/s):	0			Threshold entrainment depth (m):	0
<i>Input Parameters for 3d-DMM (SPH Version 2.0)</i>					
Density (kg/m ³):	2,200	Apparent basal friction angle between landslide debris and flow path (°):	8	Number of particles:	5,000
Source volume (m ³):	2,600	Apparent internal friction angle of landslide debris (°):	30		
Smoothing coefficient (B):	4	Turbulent coefficient (m/s ²):	500		
Note:	⁽¹⁾ When the pore pressure for friction is set to be zero, the “Friction angle (°)” in 2d-DMM is equivalent in concept to the “Apparent basal friction angle between landslide debris and flow path (°)” for 3d-DMM.				

Figure C2 shows the computed displacement of the debris front against time. With reference to the video footage that the debris travelled from chainage = 320 m to 530 m in approximately 20 - 21 seconds, it can be seen that the 3d-DMM (SPH Version 2.0) simulation run is able to meet this requirement.

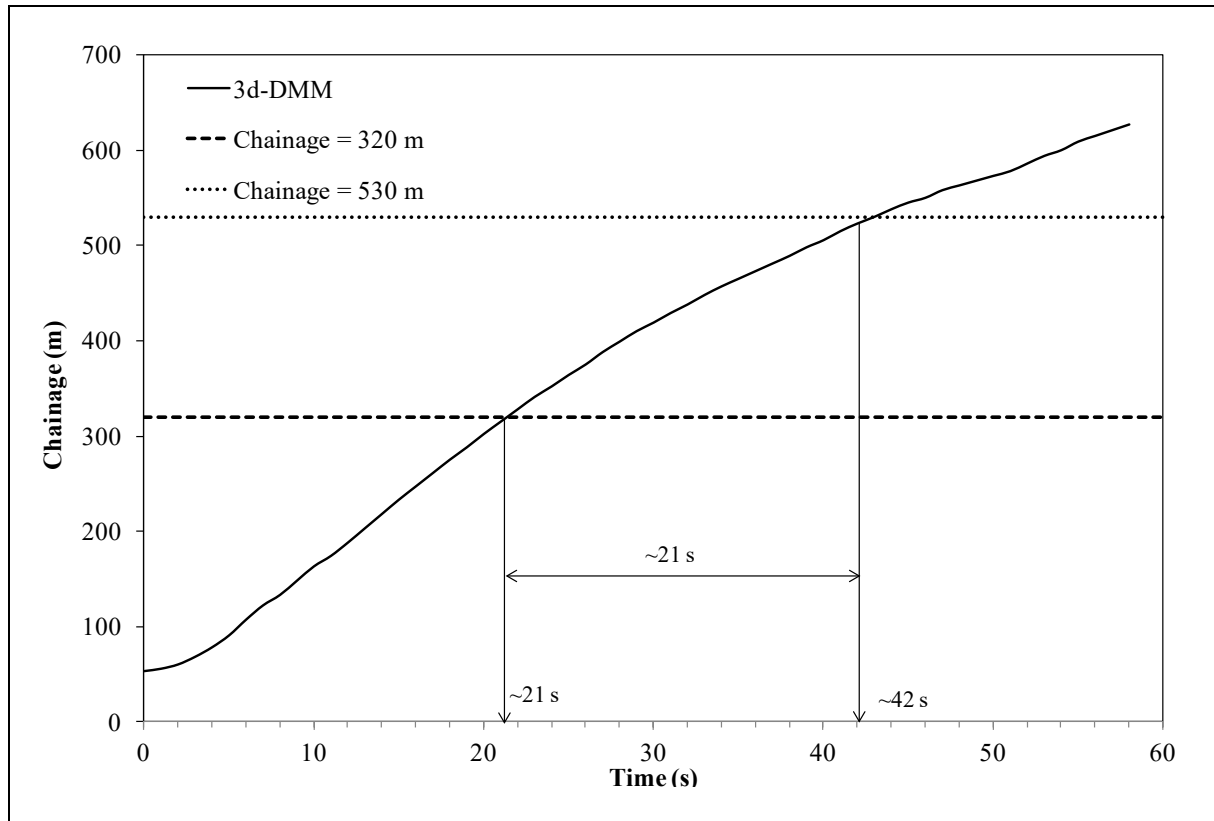


Figure C2 Debris Frontal Location versus Time Estimated by 3d-DMM (SPH Version 2.0) Analysis

Figure C3 shows the maximum velocity profiles of the landslide debris with time for Verification Case No. 1. The computed results using 3d-DMM (SPH Version 2.0) (shown in blue solid line) and DAN-3D (shown in red solid line) are presented in the figure. It is noted that the maximum velocity calculated using 3d-DMM (SPH Version 2.0) and DAN-3D match reasonably well with each other. The fluctuation in the maximum velocity calculated using DAN-3D is observed to be less than that of 3d-DMM (SPH Version 2.0), probably due to the presence of the velocity smoothing (see Section 2.4) in DAN-3D, but not in 3d-DMM (SPH Version 2.0).

References

GEO (2012). *Detailed Study of the 7 June 2008 Landslides on the Hillside above Yu Tung Road, Tung Chung (GEO Report No. 271)*. Report prepared by AECOM. Geotechnical Engineering Office, Hong Kong, 124 p.

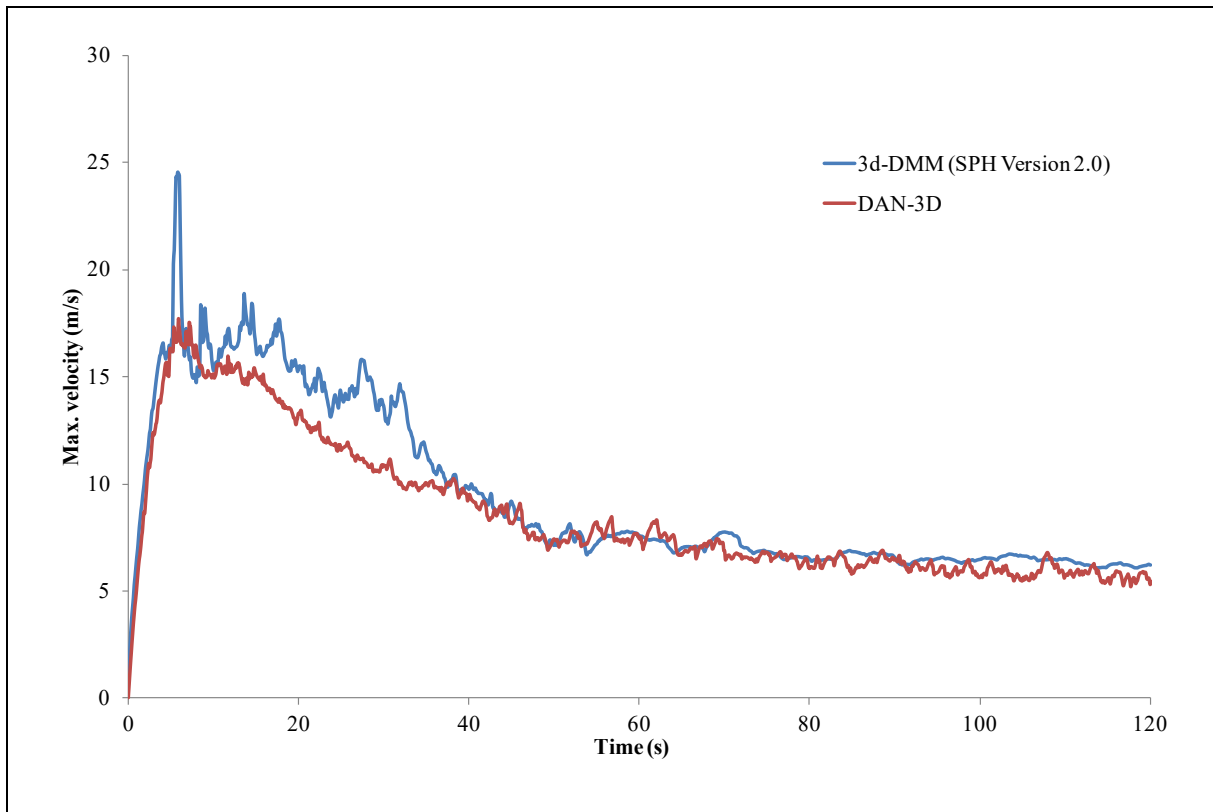


Figure C3 Comparison between the Computed Maximum Velocity Profiles Using 3d-DMM (SPH Version 2.0) and DAN-3D

C.2 Validation Case No. 2 - Sham Tseng San Tsuen Landslide

In the morning of 23 August 1999, landslides occurred on the natural hillside above Sham Tseng San Tsuen. The landslide debris, of a total volume of 600 m³, ran into a streamcourse and developed into a channelised debris flow. The debris flow demolished several dwellings at the outlet of the streamcourse.

Figure C4 shows the velocity profiles of debris front along chainage for Verification Case No. 2. Based on the superelevation level of the observed debris marked along the flow path, the velocity of the debris flow at chainage = 121 m and chainage = 217 m were about 11 m/s and 7 m/s respectively (GEO, 2005). The computed frontal velocities from 2d-DMM (Version 2.0) and 3d-DMM (SPH Version 2.0) were compared with the field observations (see also Table C2 for the input parameters). While the turbulent coefficient in both simulations were chosen to be 500 m/s², a different values of the friction angle were adopted for 2d-DMM (11°) and 3d-DMM (8°). A relatively lower value of the friction angle adopted in 3d-DMM (SPH Version 2.0) could possibly be explained by the presence of bends which slowed down the landslide debris in 3d-DMM (SPH Version 2.0). However, this retarding effects of the bends would not have been simulated by 2d-DMM, thus a larger friction angle in 2d-DMM (Version 2.0) was required to mimic the deceleration at bends. There is no computed velocity data before chainage = 20 m since the frontal debris is located close to chainage = 20 m. It is noted that the frontal velocities calculated using 2d-DMM (Version 2.0), 3d-DMM (SPH Version 2.0) and LS-DYNA match reasonably well with the field data.

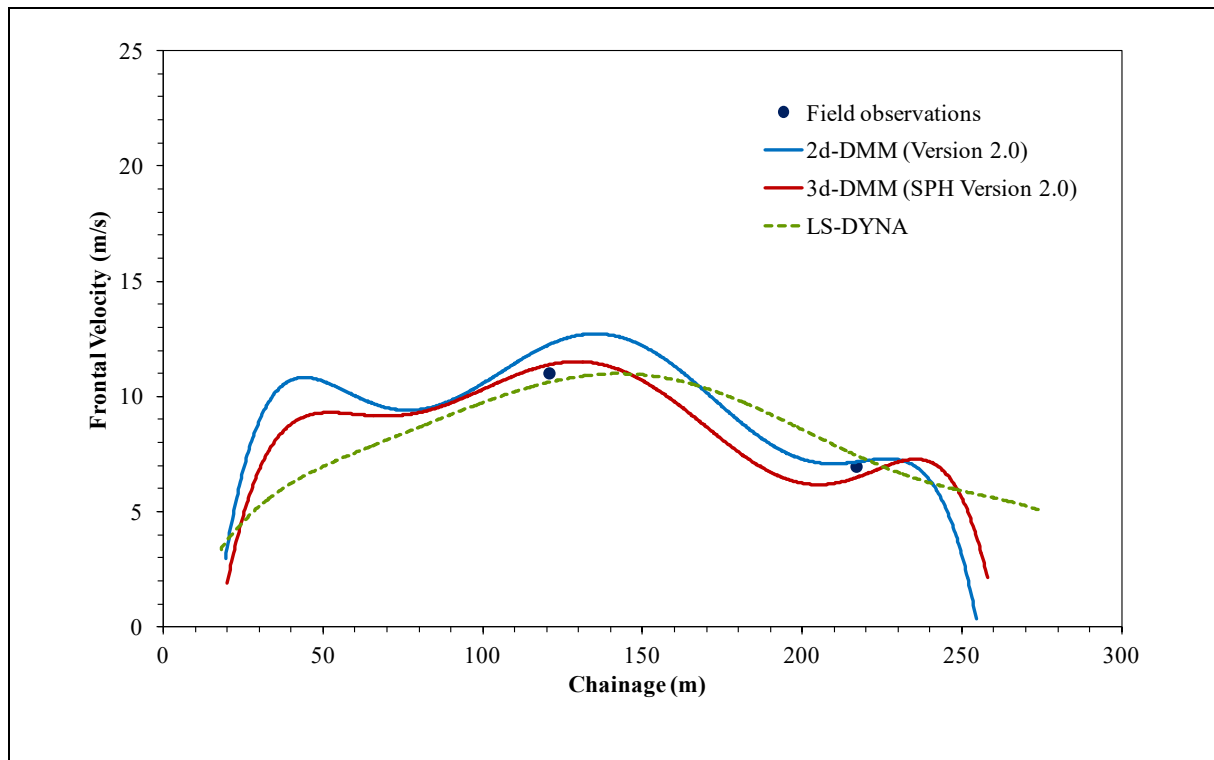


Figure C4 Comparison between the Computed Velocity Profiles Using 2d-DMM (Version 2.0), 3d-DMM (SPH Version 2.0) and Field Evidence of Debris Flow above Sham Tseng San Tsuen in August 1999

References

- GEO (2005). *Report on the Debris flow at Sham Tseng San Tsuen of 23 August 1999 (GEO Report No. 169)*. Report prepared by Fugro Maunsell Scott Wilson Joint Venture. Geotechnical Engineering Office, Hong Kong, 95 p.

Table C2 Input Parameters Adopted for the Validation Case No. 2

<i>Input Parameters for 2d-DMM (Version 2.0)</i>					
Debris Properties		Section 1			
Density (kg/m ³):	2,200	Friction angle (°):	11	Entrainment start location (m):	0
Source volume (m ³):	600	Turbulent coefficient (m/s ²):	500	Entrainment end location (m):	0
Initial horizontal length of flow mass (m):	20	Pore pressure for friction:	0	Entrainment rate (m ³ /s):	0
K_a :	0.8	Section 2			
K_θ :	1	Start location of section 2 (m):	10,000	Entrainment start location (m):	0
K_p :	2.5	Friction angle (°):	11	Entrainment end location (m):	0
Pore pressure ratio (R_u):	0.5	Turbulent coefficient (m/s ²):	500	Entrainment rate (m ³ /s):	0
Initial location of landslide debris (m):	0	Pore pressure for friction:	0		
Initial velocity (m/s):	0			Threshold entrainment depth (m):	0
<i>Input Parameters for 3d-DMM (SPH Version 2.0)</i>					
Density (kg/m ³):	2,200	Apparent basal friction angle between landslide debris and flow path (°):	8	Number of particles:	5,000
Source volume (m ³):	600	Apparent internal friction angle of landslide debris (°):	30		
Smoothing coefficient (B):	4	Turbulent coefficient (m/s ²):	500		

C.3 Validation Case No. 3 - 1990 Tsing Shan Landslide

Tsing Shan debris flow in September 1990 involved a significant entrainment behaviour throughout the transportation process. Given the availability of field evidence of flow velocity, this debris flow case is ideal to validate the capacity of 3d-DMM (SPH Version 2.0) in modelling entrainment.

According to King (2013), the debris flow was initiated by a landslide of about 350 m³. The volume of the detached landslide debris reached about 4,000 m³ at chainage = 100 m. The landslide debris subsequently developed into a debris flow through heavy entrainment along its runout path. The debris volume was increased to 20,000 m³ before reaching its final deposition. A considerable portion of the landslide deposit is located between chainage = 500 m to chainage = 700 m. Depositions of landslide debris were also observed further but King (2013) stated that the heavy rain during and after the debris flow was probably important with respect to the form of the final debris deposit and its runout distance. The field mapped runout distance may not correspond to actual debris mobility.

Superelevation data of the debris flow were recorded at chainage = 350 m and chainage = 475 m where the trail followed bends in the valley. At chainage = 350 m the average velocity calculated was 16.5 m/s and at chainage = 475 m was 12.5 m/s.

Table C3 Input Parameters Adopted for the Validation Case No. 3

<i>Input Parameters for 3d-DMM (SPH Version 2.0)</i>			
Density (kg/m ³):	2,200	Apparent basal friction angle between landslide debris and flow path (°):	15
Source volume (m ³):	4,000	Apparent internal friction angle of landslide debris (°):	30
Final volume (m ³):	20,000 ⁽¹⁾		
Smoothing coefficient (<i>B</i>):	4	Turbulent coefficient (m/s ²):	500
Number of particles:	5,000		
Note: ⁽¹⁾ An entrainment rate of 0.0035 m ⁻¹ is adopted in 3d-DMM (SPH Version 2.0).			

Being classified as a debris flow, the landslide debris is laterally confined, at least for a significant portion of the flow path, which fits with the modelling assumptions of 2d-DMM (Version 2.0). A comparison of the field evidence (i.e. velocity, major deposition between chainage = 500 m to chainage = 700 m) and computed results of 3d-DMM (SPH Version 2.0) and 2d-DMM (Version 2.0) are conducted.

Figure C5 shows the comparisons. The frontal velocities calculated using 2d-DMM (Version 2.0) and 3d-DMM (SPH Version 2.0) match reasonably well with each other, and with the field observations. A good match of the trends indicates the validity of 3d-DMM (SPH Version 2.0) in modelling entrainment.

It should be cautioned that the apparent friction angles and the turbulent coefficients adopted are different in 3d-DMM (SPH Version 2.0) ($\phi_a = 15^\circ$ and $\xi = 500 \text{ m/s}^2$) and 2d-DMM (Version 2.0) ($\phi_a = 18^\circ$ and $\xi = 700 \text{ m/s}^2$), probably due to the difference in the method of discretisation and the dimensions of the computational domain.

Figure C6(a) shows the comparison between the simulated debris profiles and the measured extent of the debris flow event (shown as the red dotted line). A significant portion of the landslide debris is deposited between chainage = 500 m to chainage = 700 m, which match with the field measurement. The extent of the simulated debris flow also agrees with the field observed extent before chainage = 700 m.

The simulated debris profiles using 3d-DMM (PIC Version) (Kwan & Sun, 2007) is given in Figure C6(b) and the computed profiles of the two computer programs are consistent.

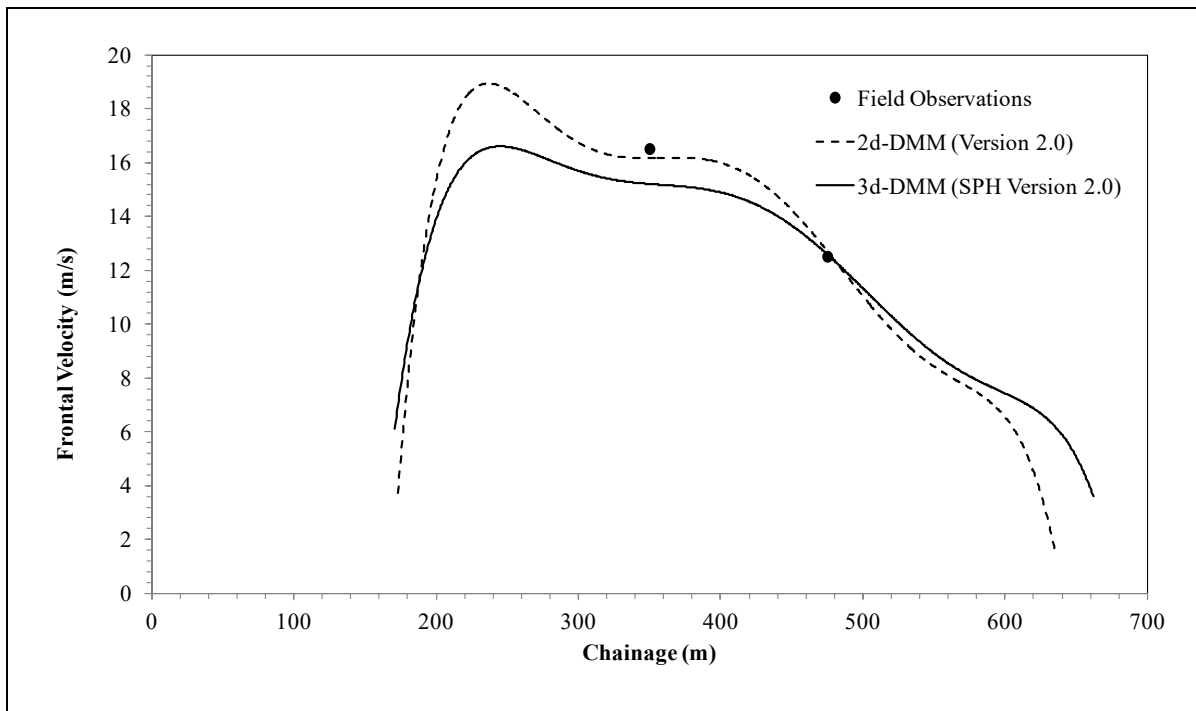


Figure C5 Comparison between the Computed Velocity Profiles Using 2d-DMM (Version 2.0), 3d-DMM (SPH Version 2.0) and Field Observation of Debris Flow on Tsing Shan in September 1990

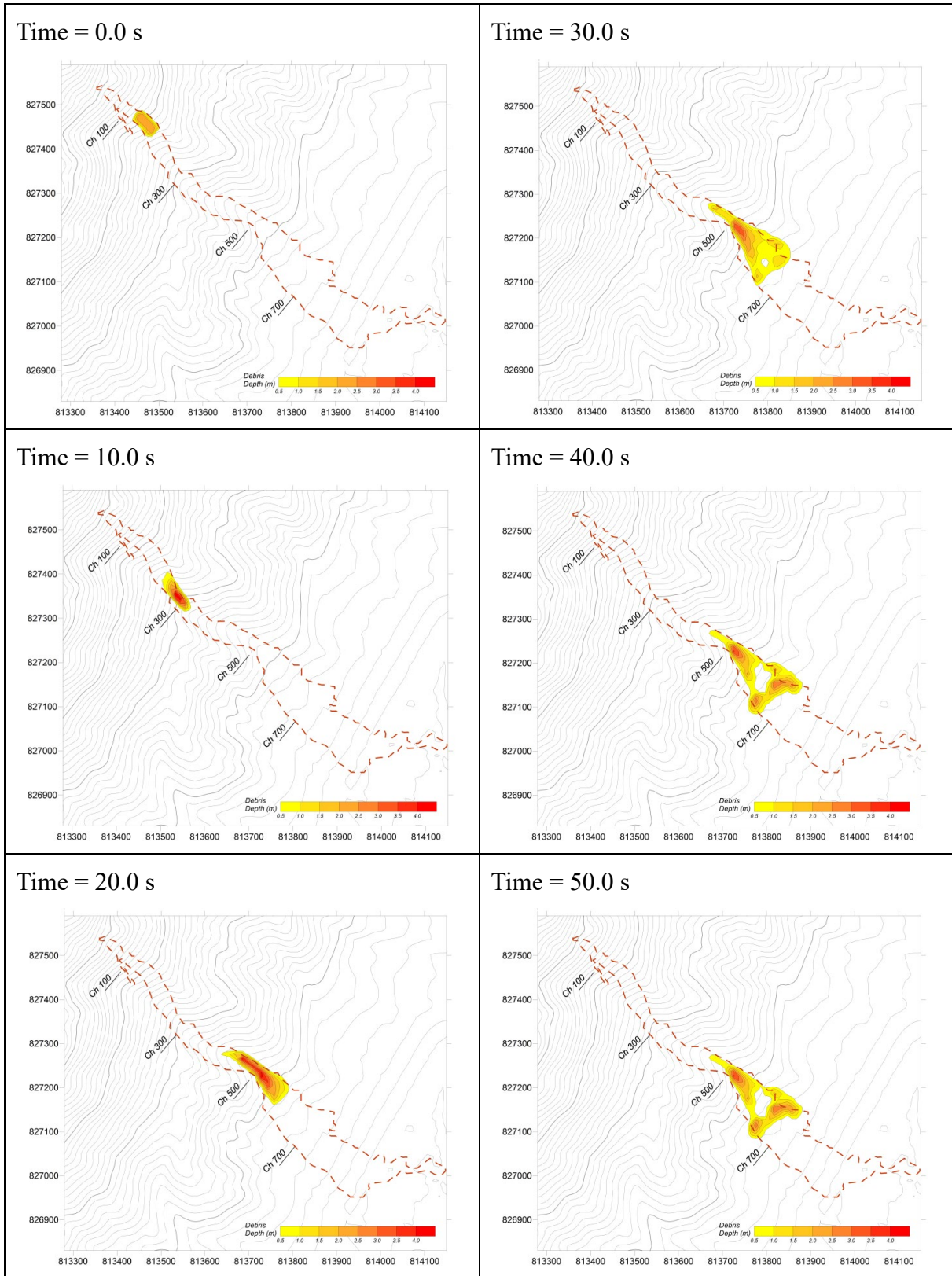


Figure C6(a) Comparison between the Field Evidence and the Simulated Debris Profiles Using 3d-DMM (SPH Version 2.0)

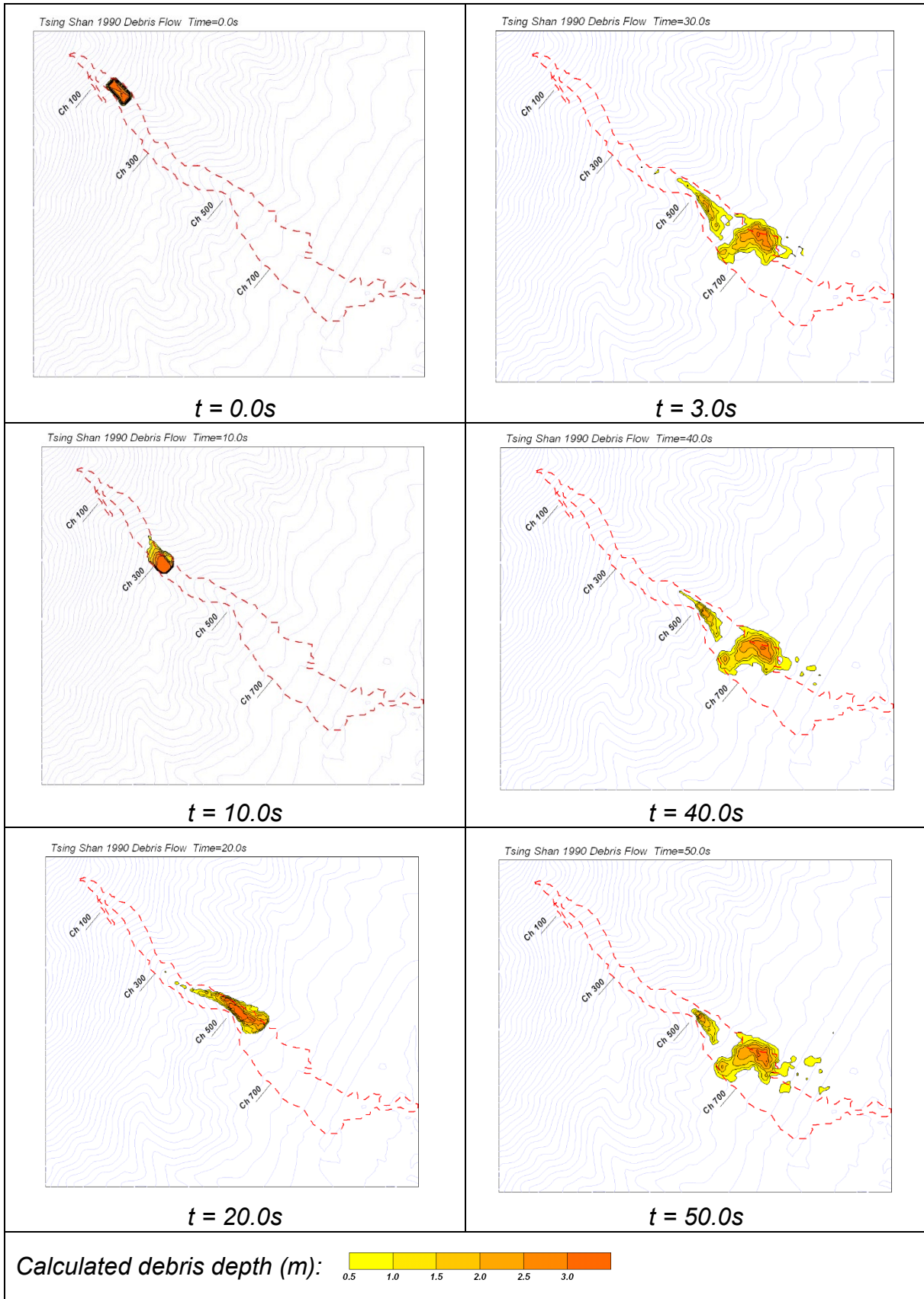


Figure C6(b) Comparison between the Field Evidence and the Simulated Debris Profiles Using 3d-DMM (PIC Version) (Kwan & Sun, 2007)

References

- King, J.P. (2013). *Tsing Shan Debris Flow and Debris Flood (GEO Report No. 281)*. Geotechnical Engineering Office, Hong Kong, 268 p.
- Kwan, J.S.H. & Sun, H.W. (2007). Benchmarking exercise on landslide mobility modelling - runout analyses using 3dDMM. *Proceedings of the International Forum on Landslide Disaster Management*, Hong Kong, vol. II, pp 945-966.

C.4 Validation Case No. 4 - Kau Lung Hang Shan Landslide

According to GEO (2006), the landslide involved an estimated failure volume of about 200 m³ from the source area. Approximately 180 m³ of the failed material detached from the source area and travelled down an ephemeral drainage line as a debris flow (20 m³ of debris was deposited within the source area). The deposition of fine grained fluvial outwash material reached the boundary of two village houses. No damage to these village houses was observed and no casualties were reported. The superelevation data of the debris flow were recorded at four chainage locations where the trail followed bends in the flow path.

The failure involved landslide debris travelling in topographic depression. A comparison between the field evidence (i.e. velocity interpreted from the superelevation data) and the computed frontal velocities profiles of the landslide debris using 3d-DMM (SPH Version 2.0) and 2d-DMM (Version 2.0) was made.

Figure C7 shows the velocity profiles of debris front along chainage for Verification Case No. 4. The computed frontal velocities from 2d-DMM (Version 2.0) and 3d-DMM (SPH Version 2.0) are compared with the field observations. Similar to Verification Case No. 2, a slightly different values of the friction angle were adopted for 2d-DMM (18° for Version 2.0) and 3d-DMM (17° for SPH Version 2.0). The same explanation (i.e. 3D analysis is able to capture the retarding effect of bends but not 2D analysis) given in Verification Case No. 2 applies equally to this verification case. The turbulent coefficient in both simulations were chosen to be 500 m/s². It is noted that the frontal velocities calculated using 2d-DMM (Version 2.0) and 3d-DMM (SPH Version 2.0) match reasonably well with each other, and with the field data.

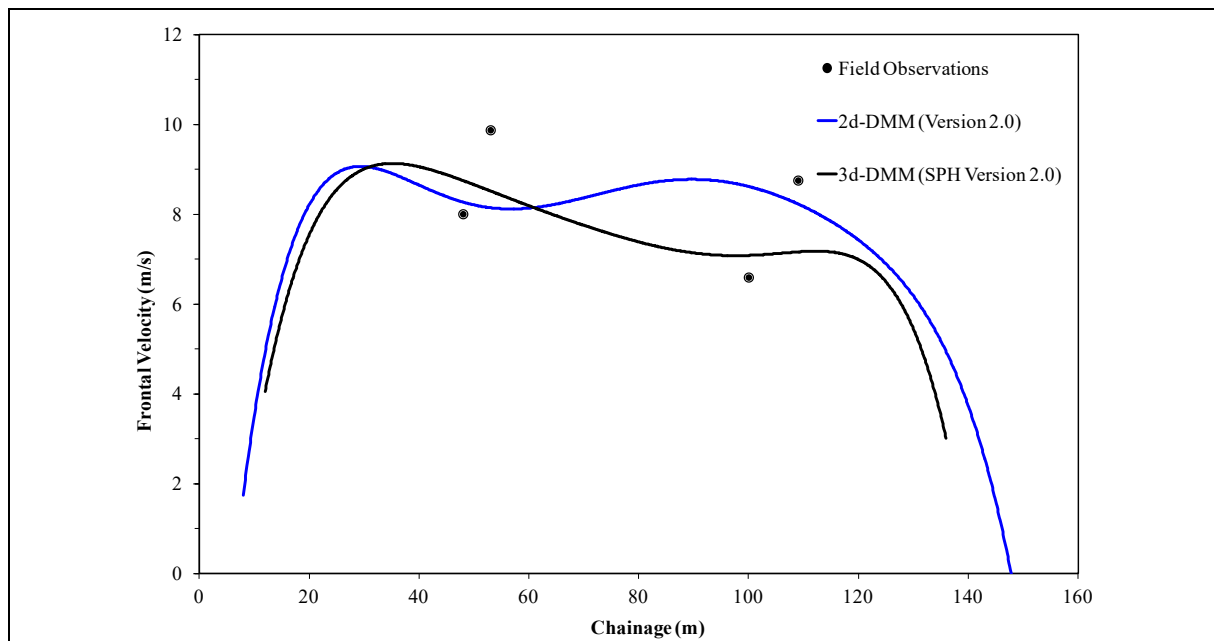


Figure C7 Comparison between the Computed Velocity Profiles Using 2d-DMM (Version 2.0), 3d-DMM (SPH Version 2.0) and Field Evidence of Debris Flow at Kau Lung Hang Shan Tai Po in 2003

Table C4 Input Parameters Adopted for the Validation Case No. 4

<i>Input Parameters for 2d-DMM (Version 2.0)</i>					
Debris Properties		Section 1			
Density (kg/m ³):	2,200	Friction angle ⁽¹⁾ (°):	18	Entrainment start location (m):	0
Source volume (m ³):	180	Turbulent coefficient (m/s ²):	1,000	Entrainment end location (m):	0
Initial horizontal length of flow mass (m):	20	Pore pressure for friction:	0	Entrainment rate (m ³ /s):	0
K_a :	0.8	Section 2			
K_θ :	1	Start location of section 2 (m):	1,000	Entrainment start location (m):	0
K_p :	2.5	Friction angle (°):	18	Entrainment end location (m):	0
Pore pressure ratio (R_u):	0.5	Turbulent coefficient (m/s ²):	1,000	Entrainment rate (m ³ /s):	0
Initial location of landslide debris (m):	0	Pore pressure for friction:	0		
Initial velocity (m/s):	0			Threshold entrainment depth (m):	0
<i>Input Parameters for 3d-DMM (SPH Version 2.0)</i>					
Density (kg/m ³):	2,200	Apparent basal friction angle between landslide debris and flow path (°):	17	Number of particles:	5,000
Source volume (m ³):	180	Apparent internal friction angle of landslide debris (°):	30		
Kernel length (m):	4	Turbulent coefficient (m/s ²):	1,000		
Note:	⁽¹⁾ When the pore pressure for friction is set to be zero, the “Friction angle (°)” in 2d-DMM is equivalent in concept to the “Apparent basal friction angle between landslide debris and flow path (°)” for 3d-DMM.				

References

GEO (2006). *The 5 May 2003 Debris Flow at Kau Lung Hang Shan Tai Po (GEO Report No. 196)*. Report prepared by Maunsell Geotechnical Services Limited. Geotechnical Engineering Office, Hong Kong, 84 p. plus 1 drg.

C.5 Validation Case No. 5 - Fei Tsui Road Landslide

The landslide occurred on a man-made cut slope along Fei Tsui Road, Hong Kong. The landslide investigation revealed that there was an extensive kaolinite-rich layer on the base of the landslide scar dipping towards Fei Tsui Road. Within the landslide source area, a low base friction angle of 22° was used to account for the presence of the kaolinite-rich layer. In contrast, a higher base friction angle of 35° was used for movement of the landslide debris over Fei Tsui Road. The measured deposit profiles (GEO, 1996) were compared with the computed deposit profiles by 3d-DMM (SPH Version 2.0), as well as the computed deposit profile computed using 3d-DMM (PIC Version) (Kwan & Sun, 2007) and LS-DYNA (Koo, 2015).

Table C5 Input Parameters Adopted for the Validation Case No. 5

<i>Input Parameters for 3d-DMM (SPH Version 2.0)</i>			
Density (kg/m^3):	2,200	Apparent basal friction angle between landslide debris and flow path ($^\circ$):	22 35 ⁽¹⁾
Source volume (m^3):	14,000	Apparent internal friction angle of landslide debris ($^\circ$):	30
Smoothing coefficient (B):	4	Turbulent coefficient (m/s^2):	0 ⁽²⁾
Number of particles:	5,000		
Notes: (1) The apparent friction angle = 22° for landslide source area and 35° for movement of the landslide debris over Fei Tsui Road.			
(2) The friction model is adopted in the simulation.			

Figure C8 shows the comparison between the simulated debris profiles and the field evidence (shown as the red dotted line). The simulated debris deposit spreads across Fei Tsui Road by an extent which match with the site measurement (i.e. red lines in the figure). The deposit extent simulated using 3d-DMM (SPH Version 2.0) also matches reasonably well with that by Kwan & Sun (2007) and Koo (2015).

Figure C9 shows a comparison of the computed velocity and thickness of landslide debris reaching the southern corner of the opposite church building with time. The velocity reaching the corner was calculated in 3d-DMM (SPH Version 2.0) by the average velocity of smoothed particles that were within 5 m of the location of the corner. The average velocity was only recorded when the number of smoothed particles exceed 20 as recommended by McDougall & Hungr (2004). The velocity profiles calculated using the three codes match well and the thickness calculated using 3d-DMM (SPH Version 2.0) and 3d-DMM (PIC Version) are in general comparable. The thickness calculated using LS-DYNA is larger than that of 3d-DMM (SPH Version 2.0) and 3d-DMM (PIC Version).

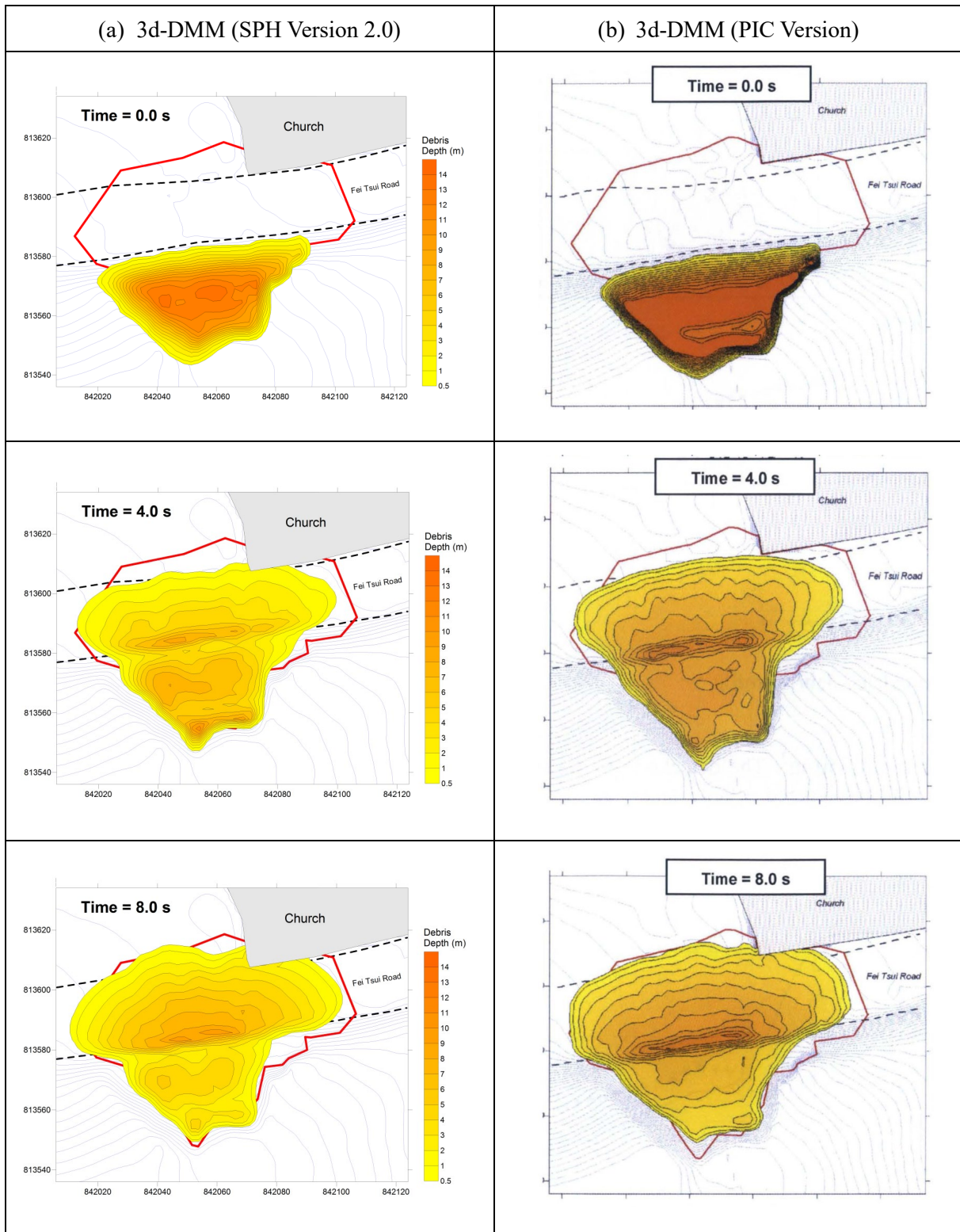


Figure C8 Comparison between the Field Evidence (red lines) and the Simulated Debris Profiles Using 3d-DMM (SPH Version 2.0) and 3d-DMM (PIC Version) (Kwan & Sun, 2007)

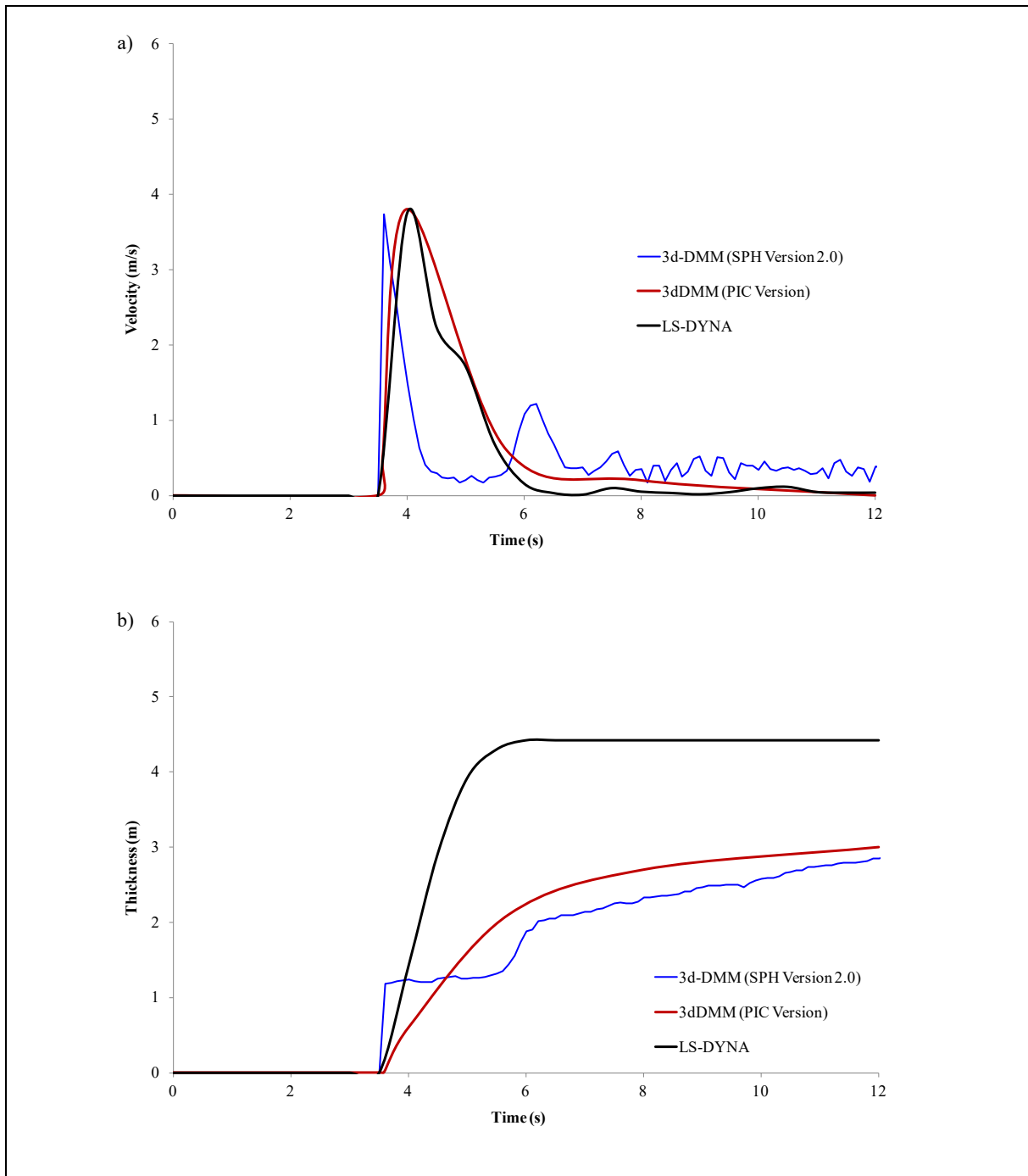


Figure C9 Comparison of Velocity and Thickness of Debris of Fei Tsui Road Landslide Reaching the Southern Corner of the Opposite Church Building with Time

References

- GEO (1996). *Report on the Fei Tsui Road Landslide of 13 August 1995, Volume 2*. Geotechnical Engineering Office, Hong Kong, 69 p.
- Koo, R.C.H. (2015). *3D Debris Mobility Assessment Using LS-DYNA (SPR No. 4/2015)*. Geotechnical Engineering Office, Hong Kong, 87 p.
- Kwan, J.S.H. & Sun, H.W. (2007). Benchmarking exercise on landslide mobility modelling - runout analyses using 3dDMM. *Proceedings of the International Forum on Landslide Disaster Management*, Hong Kong, vol. II, pp 945-966.
- McDougall, S. & Hungr, O. (2004). A model for the analysis of rapid landslide motion across three-dimensional terrain. *Canadian Geotechnical Journal*, vol. 41, pp 1084-1097.

C.6 Validation Case No. 6 - Shum Wan Landslide

The Shum Wan Landslide involved a landslide mass of 26,000 m³. It occurred on a 30° natural hillside during heavy rainfall. A planar, slab-like ground mass detached and slid down from the hillside and the landslide debris was stopped after hitting a shipyard at the slope toe. Site observations suggested that the landslide mass might remain intact during the sliding process. The measured deposit profiles (GEO, 1996) was compared with the computed deposit profiles by 3d-DMM (SPH Version 2.0), as well as the computed deposit profile computed using 3d-DMM (PIC Version) (Kwan & Sun, 2007) and LS-DYNA (Koo, 2015).

Table C6 Input Parameters Adopted for the Validation Case No. 6

<i>Input Parameters for 3d-DMM (SPH Version 2.0)</i>			
Density (kg/m ³):	2,200	Apparent basal friction angle between landslide debris and flow path (°):	19
Source volume (m ³):	26,000	Apparent internal friction angle of landslide debris (°):	33
Kernel length (m):	4	Turbulent coefficient (m/s ²):	0 ⁽¹⁾
Number of particles:	5,000		
Note: ⁽¹⁾ The friction model is adopted in the simulation.			

Figures C10 and C11 show the simulated deposit profiles. The extent of the landslide affected zone is also shown on the figures. The simulated debris deposit spreads across the shipyard by an extent which matches reasonably well with the site observation (i.e. red lines in the figure). Also, the deposit extent simulated using 3d-DMM (SPH Version 2.0) also matches with that by Kwan & Sun (2007) and Koo (2015).

The values of the apparent internal friction angle adopted in the back analysis of the Verification Case No. 1 to 3 are equal to 30°. In this Verification Case, however, a slightly higher apparent internal friction angle, 33°, was required for a close match with the measured deposit profile. Apparent internal friction angle reduces the spreading of the landslide debris deposition. The larger required internal friction angle possibly represents the resistance against the landslide debris motions given by the shipyard structures.

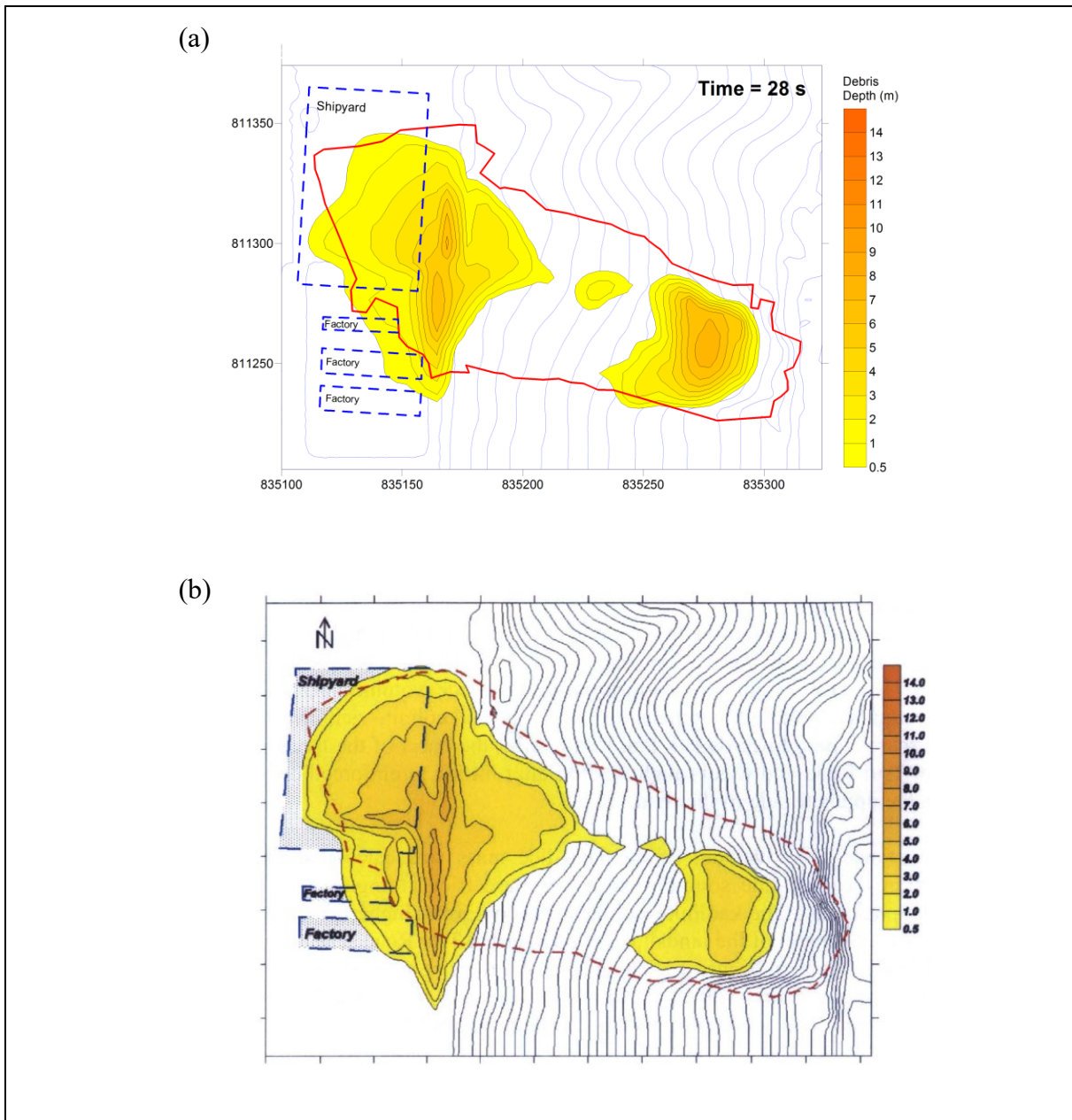


Figure C10 Comparison between the Field Evidence (red lines) and the Simulated Debris Profiles Using (a) 3d-DMM (SPH Version 2.0) and (b) 3d-DMM (PIC Version) (Kwan & Sun, 2007)

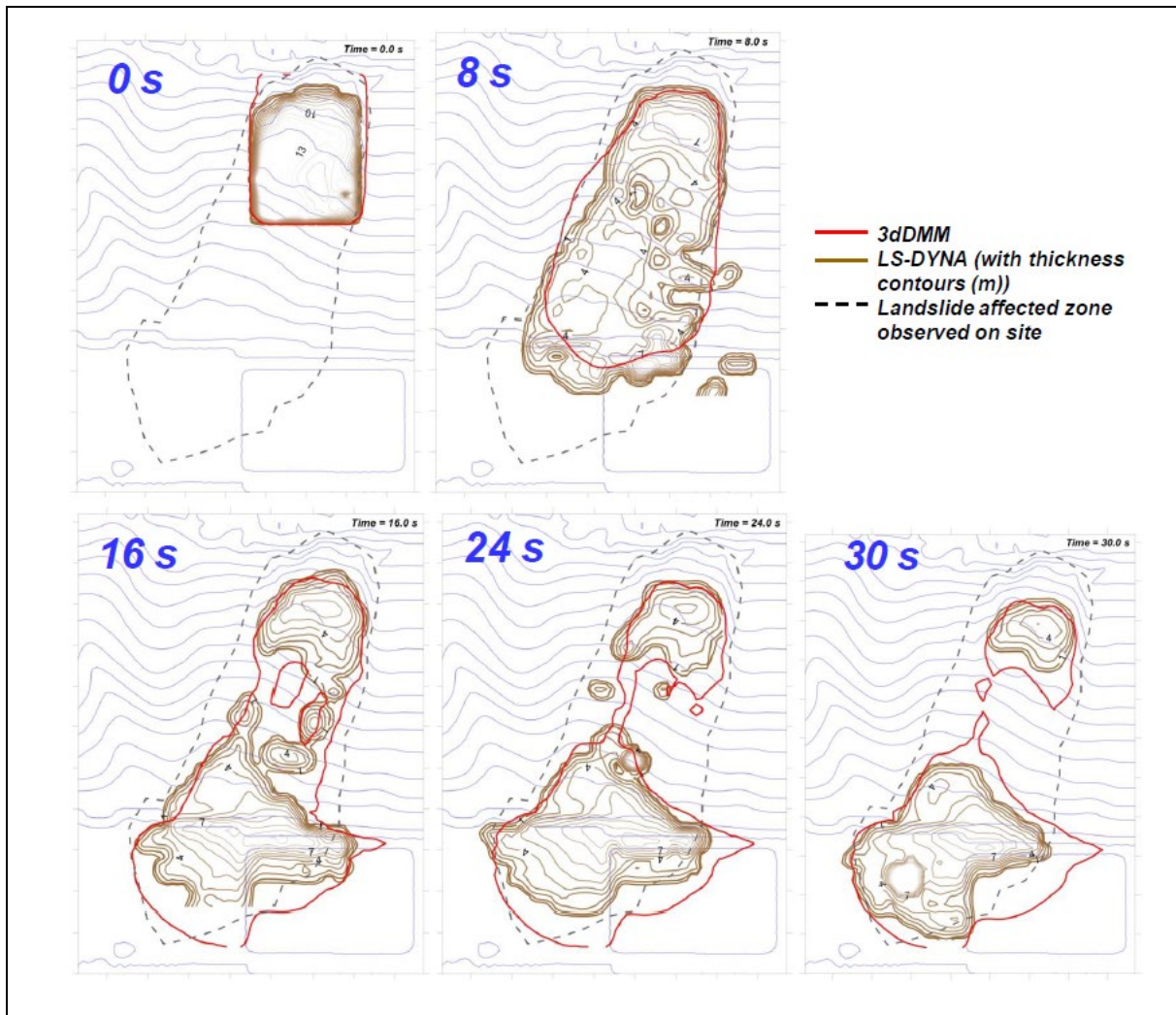


Figure C11 Comparison of Simulations between LS-DYNA and 3d-DMM (PIC Version) (Koo, 2015)

References

- GEO (1996). *Report on the Shum Wan Road Landslide of 13 August 1995, Volume 2*. Geotechnical Engineering Office, Hong Kong, 52 p.
- Koo, R.C.H. (2015). *3D Debris Mobility Assessment Using LS-DYNA (SPR No. 4/2015)*. Geotechnical Engineering Office, Hong Kong, 87 p.
- Kwan, J.S.H. & Sun, H.W. (2007). Benchmarking exercise on landslide mobility modelling - runout analyses using 3dDMM. *Proceedings of the International Forum on Landslide Disaster Management*, Hong Kong, vol. II, pp 9.

GEO PUBLICATIONS AND ORDERING INFORMATION

土力工程處刊物及訂購資料

An up-to-date full list of GEO publications can be found at the CEDD Website <http://www.cedd.gov.hk> on the Internet under "Publications". The following GEO publications can also be downloaded from the CEDD Website:

- i. Manuals, Guides and Specifications
- ii. GEO technical guidance notes
- iii. GEO reports
- iv. Geotechnical area studies programme
- v. Geological survey memoirs
- vi. Geological survey sheet reports

Copies of some GEO publications (except geological maps and other publications which are free of charge) can be purchased either by:

Writing to

Publications Sales Unit,
Information Services Department,
Room 626, 6th Floor,
North Point Government Offices,
333 Java Road, North Point, Hong Kong.

or

- Calling the Publications Sales Section of Information Services Department (ISD) at (852) 2537 1910
- Visiting the online Government Bookstore at <http://www.bookstore.gov.hk>
- Downloading the order form from the ISD website at <http://www.isd.gov.hk> and submitting the order online or by fax to (852) 2523 7195
- Placing order with ISD by e-mail at puborder@isd.gov.hk

1:100 000, 1:20 000 and 1:5 000 geological maps can be purchased from:

Map Publications Centre/HK,
Survey & Mapping Office, Lands Department,
23th Floor, North Point Government Offices,
333 Java Road, North Point, Hong Kong.
Tel: (852) 2231 3187
Fax: (852) 2116 0774

Any enquires on GEO publications should be directed to:

Chief Geotechnical Engineer/Standards and Testing,
Geotechnical Engineering Office,
Civil Engineering and Development Department,
Civil Engineering and Development Building,
101 Princess Margaret Road,
Homantin, Kowloon, Hong Kong.
Tel: (852) 2762 5351
Fax: (852) 2714 0275
E-mail: ivanli@cedd.gov.hk

詳盡及最新的土力工程處刊物目錄，已登載於土木工程拓展署的互聯網網頁<http://www.cedd.gov.hk> 的“刊物”版面之內。以下的土力工程處刊物亦可於該網頁下載：

- i. 指南、指引及規格
- ii. 土力工程處技術指引
- iii. 土力工程處報告
- iv. 岩土工程地區研究計劃
- v. 地質研究報告
- vi. 地質調查圖表報告

讀者可採用以下方法購買部分土力工程處刊物(地質圖及免費刊物除外):

書面訂購

香港北角渣華道333號
北角政府合署6樓626室
政府新聞處
刊物銷售組

或

- 致電政府新聞處刊物銷售小組訂購 (電話：(852) 2537 1910)
- 進入網上「政府書店」選購，網址為 <http://www.bookstore.gov.hk>
- 透過政府新聞處的網站 (<http://www.isd.gov.hk>) 於網上遞交訂購表格，或將表格傳真至刊物銷售小組 (傳真：(852) 2523 7195)
- 以電郵方式訂購 (電郵地址：puborder@isd.gov.hk)

讀者可於下列地點購買1:100 000、1:20 000及1:5 000地質圖：

香港北角渣華道333號
北角政府合署23樓
地政總署測繪處
電話: (852) 2231 3187
傳真: (852) 2116 0774

如對本處刊物有任何查詢，請致函：

香港九龍何文田公主道101號
土木工程拓展署大樓
土木工程拓展署
土力工程處
標準及測試部總土力工程師
電話: (852) 2762 5351
傳真: (852) 2714 0275
電子郵件: ivanli@cedd.gov.hk